

# Are galaxy distributions scale invariant?

A perspective from dynamical systems theory

J.L. McCauley\*  
Sektion Physik  
Universität München  
Theresienstr. 37 D-80333 München  
★ Permanent Address:  
Physics Department,  
University of Houston,  
Houston, Texas 77204

March 7, 1997

## Abstract

Unless there is evidence for fractal scaling with a single exponent over distances  $.1 \leq r \leq 100h^{-1}\text{Mpc}$  then the widely accepted notion of scale invariance of the correlation integral for  $.1 \leq r \leq 10h^{-1}\text{Mpc}$  must be questioned. The attempt to extract a scaling exponent  $\nu$  from the correlation integral  $n(r)$  by plotting  $\log(n(r))$  vs.  $\log(r)$  is unreliable unless the underlying point set is approximately monofractal. The extraction of a spectrum of generalized dimensions  $\nu_q$  from a plot of the correlation integral generating function  $G_n(q)$  by a similar procedure is probably an indication that  $G_n(q)$  does not scale at all. We explain these assertions after defining the term multifractal, mutually-inconsistent definitions having been confused together in the cosmology literature. Part of this confusion is traced to a misleading speculation made earlier in the dynamical systems theory literature, while other errors follow from confusing together entirely different definitions of “multifractal” from two different schools of thought. Most important are serious errors in data analysis that follow from taking for granted a largest term approximation that is inevitably advertised in the literature on both fractals and dynamical systems theory.

## 1 Introduction

Knowledge of the three-dimensional distribution of matter in the universe at  $r > 150h^{-1}\text{Mpc}$  is limited. We do not know if the matter distribution over scales  $r \gg 150h^{-1}\text{Mpc}$  is homogeneous or isotropic (background radiation, self-consistency of the standard model based on the assumption of a *stable* uniform density, etc. do not provide direct evidence about the distribution of visible matter in the present epoch). For  $r < 150h^{-1}\text{Mpc}$  the distribution of visible matter is clearly inhomogeneous, with large voids and clustering, and various analyses have produced results that are equivalent to claiming scale invariance for the correlation integral, that  $n(r) \approx r^\nu$ , with one school ([17], [61]) reporting that  $\nu \approx 1.23$  for  $.1 < r < 10h^{-1}\text{Mpc}$ , whereas the other ([13], [6]) reports that  $\nu \approx 2$  for  $2 < r < 150h^{-1}\text{Mpc}$ . The correlation integral and scaling exponent  $\nu$  are defined in part 4. Roughly speaking, one can think of the scaling exponent  $\nu$  as a correlation dimension, but not as Hausdorff or box-counting dimension. We will explain why the reported claims of scale invariance may be spurious unless the matter distribution actually is, to a very good approximation, monofractal. The first aim of this paper is to explain the need for a more careful analysis of observational data than has heretofore been performed. The second aim is to provide that analysis (part 5). The third is to explain and eliminate the confusion over the term

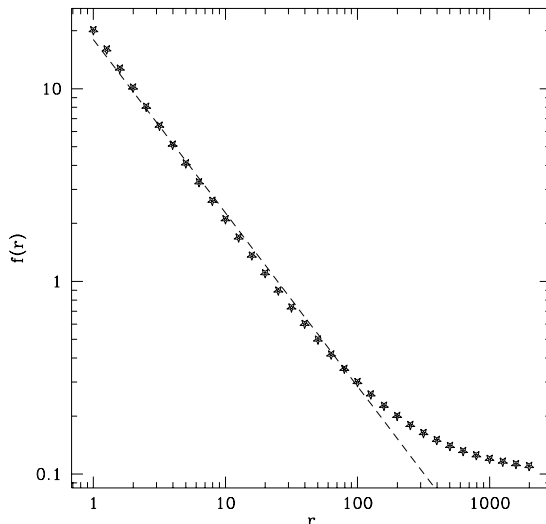


Figure 1: Log–log plot of a function  $f(r) = 20 r^{-\gamma_1} + 0.1 r^{-\gamma_2}$  (stars), with  $\gamma_1 = 1$  and  $\gamma_2 = 0$  together with the function  $18 r^{-\gamma_3}$  (dashed line) with  $\gamma_3 = 0.9$ .

multifractal. Finally we will explain why a “nonanalytic” density does not rule out the use of differential equations.

In any attempt to extract scaling exponents from log–log plots of correlation or generating functions a conservative criterion in both critical phenomena and dynamical systems theory is that linearity should be exhibited over at least three decades, which would require data out to at least  $r = 1000 h^{-1}\text{Mpc}$  in astronomy. The reason for this is that there are too many different functions  $f(r)$  that don’t scale with  $r$ ,  $f(\lambda r) \neq \lambda^\alpha f(r)$ , but  $\log(f(r))$  vs.  $\log(r)$  may nevertheless *appear* to have a constant slope over a short enough range of  $r$ . The function  $f(r) = c_1 r^a + c_2 r^b$  provides a relevant example: this function is not scale invariant because of *two* exponents  $a$  and  $b$ , but it is easy to exhibit the *illusion* of scale invariance by plotting  $\log(f(r))$  vs.  $\log(r)$  over only two decades (see figure 1). If one questions the controversial claim of scale invariance over two decades up to  $r \approx 150 h^{-1}\text{Mpc}$ , then must also one question the *widely accepted* claim of scale invariance, *also* over only two decades, up to  $r \approx 10 h^{-1}\text{Mpc}$ .

To make our viewpoint clear to the reader we recapitulate briefly the controversy over scaling in this field. The earliest attempts to extract  $\nu$  were based upon the expectation of homogeneity at larger scales, with inhomogeneities confined to  $r \leq r_0$  where  $r_0$  is a correlation length. By confusing an amplitude with a correlation (i.e. characteristic) length [17]  $r_0 \sim 5 h^{-1}\text{Mpc}$  was obtained, which is inconsistent with the observed clustering and voids out to  $r \approx 150 h^{-1}\text{Mpc}$ , and beyond. Coleman and Pietronero [13] and Martinez et al. [47] have argued instead that the known data are scale invariant, and correspondingly that there is no correlation length. Early attempts to dismiss this point of view as the result of “large deviations” due to “unfair samples” failed when it became clear that the apparent scale invariance is the rule and not the exception. As a 0<sup>th</sup> order description this seems to be correct, but we show in part 5 that a refinement of the method of [13] (see part 4) leads to the conclusion that the data are inadequate to draw a conclusion for or against multifractal scaling, although it is clear that simple fractal scaling, with a single exponent  $\nu$  as claimed by the Pietronero school, is not indicated by the data. Fractal or not, it is clear that there is, as yet, no evidence from galaxy redshift surveys of any crossover to homogeneity.

## 2 Why should anything scale?

This is a good question because, as one expert in statistical mechanics and nonlinear dynamics put it, if you can't calculate anything then you can still talk about scaling. Furthermore, most phenomena in nature do not scale, or at least have not been shown to scale (the polls are not yet closed on the question of multifractal scaling in the inertial ([1]; [12]) and dissipation ([56] & [57]) ranges of fluid turbulence, and the early returns are not entirely convincing). In fact, there are only a few known reasons why anything should scale, aside from dimensional analysis (Reynolds number scaling, which works pretty well in fluid mechanics so long as one sticks to qualitative considerations and does not look hard at the numbers). Let us enumerate the (known) ways.

First, there is scaling of all sorts of correlation functions and other thermodynamic quantities if you are close enough (within  $(T - T_c)/T_c$  of  $10^{-3}$ , at least) to a second order phase transition. The problem with this is first that the universe is not in thermodynamic equilibrium (tde): nonuniformities like spiral galaxies and DNA are not generated systematically at small scales in a system in tde. Second, there is no reason why the universe should be tuned precisely to a critical point (where  $T \approx T_c$ ). Critical phenomena are popular because the scaling indices are universal, depending only on symmetry and dimension, which allows a theorist to forget about worse details than those that plague experimentalists and calculate the scaling indices of real ferromagnets, for example, by using Ising models or  $\phi^4$  models ([32]).

We can also consider dynamical critical phenomena, where universality classes can still be defined for scaling exponents based only on symmetry and dimension, but that doesn't help: we are still restricted to systems that have only very small deviations from thermal equilibrium. Large excursions from tde aren't allowed at small scales in these systems.

Galaxies have been modelled on the basis of critical phenomena far from tde by using a particular cellular automaton ([76]) near the percolation threshold. Nice patterns can be produced that look like spiral galaxies ([68]), but who tunes the galactic system to stay near the percolation threshold? This model doesn't yet have enough physics in it to be falsifiable.

For those who believe that scaling is ubiquitous in nature, but don't expect that Mother Nature tunes phenomena to a critical point, there is SOC (self-organized criticality). The idea of SOC ([4]) is based on driven dissipative dynamical systems far from equilibrium that quite naturally lie at a borderline of chaos, for a large range of parameter values, and therefore require no parameter-tuning. Criticality (a borderline of chaos) means that all Liapunov exponents must vanish (some positive exponents are usually allowed in the literature because models where all of them vanish for a *finite* range of control parameter values ([18]) are unknown). Scaling exponents in SOC are argued to be universal because they are expected to be parameter-independent. The main problem with SOC is that no one has yet found an example of a dynamical system where the idea has been realized, criticality without parameter tuning, criticality that persists while parameters are varied. The SOC idea is usually illustrated by a sandpile model that has no tunable parameters because the parameters in the model were *implicitly* tuned to criticality and then forgotten. SOC purports to provide a universal explanation of fractal scaling indices which, if we follow the scaling enthusiasts, should be ubiquitous in nature, but *fractal and multifractal exponents are not universal and can't be used to define universality classes*. The different models used to try to describe the (still inadequate) data on the inertial and dissipation ranges of fluid turbulence provide examples of this ([51] & [55]). Sandpile models of SOC reproduce certain qualitative features of block spring models of earthquakes, but the block spring models do not produce the parameter-independent criticality demanded by SOC ([15]). SOC has not been defined unambiguously because universality classes for SOC have not been defined. In the absence of universality classes one cannot claim that a simple automaton like the sandpile model represents a complicated or complex dynamical system that occurs in nature ([55]).

Then, there are the fractals that are generated in the phase spaces of critical and *chaotic driven-dissipative* dynamical systems far from thermal equilibrium. The scaling indices that describe the fractals that occur in chaos are *not universal*. That's ok, because while the fractal dimensions are parameter-dependent the fractals persist (in distorted form) as the parameters are varied over relatively wide ranges (this is usually what happens in "SOC" models too). Given

the coarsegrained fractal support generated by a driven–dissipative dynamical system (“support” of a distribution is defined in part 3.5), nonuniform distributions on that support are typically multifractal, meaning that the coarsegrained density becomes more and more spiky (and perhaps also intermittent with voids) as the distribution is resolved at finer and finer scales of observation. The corresponding densities would be nearly everywhere nondifferentiable if the mathematicians’ fiction of an infinite–precision limit were not ruled out empirically.

Conservative dynamical systems (like gravity without dissipation/driving) cannot generate fractals in phase space: the support of any distribution generated by a conservative dynamical system is space–filling (Liouville’s theorem). Space–filling means that the support has the dimension of the phase space, whereas a fractal support has a nonintegral dimension less than that of the phase space. However, a conservative dynamical system far from thermal equilibrium can also generate multifractal coarsegrained distributions on the space–filling support. *A noninteger correlation integral scaling exponent  $\nu$  does not suggest that the galaxy distribution has a fractal support: noninteger  $\nu$  is consistent with multifractal distributions on space–filling supports.*

The problem with all of this is that it does not explain anything, as yet: the fractals and multifractals discussed above all occur in the very high dimensional phase space of all of the galaxies (each galaxy is treated as a point particle here and below), and we do not know how those distributions would look when projected onto the three dimensional space of observation in astronomy. In other words, we don’t have a quantitative explanation for where fractal (including multifractal) galaxy clusters should come from. In practice, it makes more sense to consider hydrodynamic models of galaxy formation and clustering. Hydrodynamics demands a coarsegrained description of the density. Coarsegrained descriptions are precisely what are provided by the multifractal formalism (see Vergassola et al. [75] and references therein for a hydrodynamic approach to clustering and voids). Unable at this time to contribute to the dynamical theory of galaxy formation, let us forget temporarily that no theorist can yet convincingly explain the origin of fractal galaxy clustering, if it exists, and turn instead to the question how astronomical data should be analyzed in order to decide the much easier question *whether* fractal clustering is indicated by the observational data.

## 3 Coarsegraining and fractals

### 3.1 Clustering, voids, and efficient partitions

In what follows we consider only finitely many data points  $N$  in some space, the observational data. To present the ideas in the clearest possible way we assume that the space is one–dimensional (excepting section 4 on the correlation integral, where the dimension of space is irrelevant). The ideas of sections 3.1–3.3 are admittedly heuristic and can only be made rigorous by the use of generating partitions found in the phase space of certain nonintegrable dynamical systems ([16]). In particular the heuristic description is limited to one dimension (generating partitions are not so limited), but our one dimensional treatment is adequate to the purpose of resolving the prevailing confusion over “multifractals” and “nonanalytic” densities.

We assume that the  $N$  data points in our one dimensional space are confined to the unit interval, because any finite interval can be converted into the unit interval by rescaling. With lengths denoted by  $l$ ,  $0 < l < 1$  in all that follows (planar and three dimensional cosmological data are also assumed to be rescaled so that  $0 < r < 1$  in the discussion of part 4).

Coarsegraining of the data set requires only that we cover the  $N$  points by  $N_n$  nonoverlapping intervals of size  $l^{(n)}$ . Clearly, we can take  $N_n = 2^n$  intervals of size  $l^{(n)} = 2^{-n}$ ,  $N_n = 10^n$  intervals of size  $l^{(n)} = 10^{-n}$ , and so on. All that is required to avoid overlap is  $l^{(1)} \leq 1/2$ ; coarsegraining per se is not unique. The only other requirement, so far, is that we must choose the intervals so that  $l^{(n)} \geq l_{\min}$  where  $l_{\min}$  is the smallest distance between two points in the sample (a single point cannot be coarsegrained, so that an interval containing only one point is meaningless). We shall see that the desire of the theorist to approximate  $l_{\min}$  by  $\epsilon$ , where  $\epsilon$  goes to zero, has led to serious errors in data analysis. In our analysis  $l_{\min}$  is always finite because it contains at least two

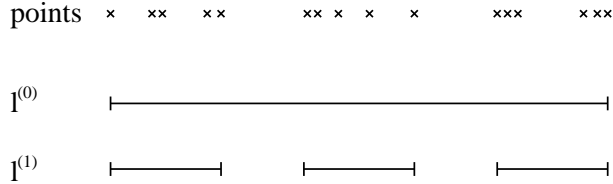


Figure 2: Nonuniform clustering with uniform partitionings. Here is no way to construct an efficient, uniform coarsegraining  $l^{(2)}$ .

real data points.

In any efficient coarsegraining the intervals that cover the points must be *nonoverlapping*, Coarsegrainings that are space-filling (meaning that  $N_n l^{(n)} = 1$ ) satisfy this criterion but do not separate voids from clusters. For data with voids we should construct a coarsegraining that is not space-filling, one where  $N_1 l^{(1)} < 1$ , in order to cover all of the clusters while excluding the largest voids. Such a coarsegraining is more efficient than an arbitrary one. With the desire for efficiency in mind the idea is first to remove all of the largest voids. Then we choose the interval size  $l^{(1)} \approx (1 - \sum v_{1,i})/N_1$ , where the intervals  $v_{1,i}$ , all of roughly the same characteristic size, represent the  $M_1$  largest voids in the sample, and  $N_1 = M_1 + 1$ . The  $N_1$  first generation intervals required to cover the  $N$  data points are not space-filling because  $N_1 l^{(1)} < 1$ , by construction. If, beneath the  $N_1$  intervals now covering the data, there are still voids and clustering then we can continue systematically by removing all voids of next largest characteristic size: in the second generation of coarsegraining simply choose  $N_2$  intervals of size  $l^{(2)} \approx (1 - \sum v_{2,i})/N_2$  where the intervals  $v_{2,i}$  represent the sizes of  $M_2$  largest voids covered by the  $N_1$  intervals  $l^{(1)}$ . This iterative procedure may be continued so long as we can distinguish clusters from voids. There are two ways that it can terminate. Either we reach a scale  $l^{(n)} > l_{\min}$  where the points are relatively evenly spaced over those intervals (so that there is no longer a distinction between clusters and voids), or else clustering continues all the way down to the finite limit  $l^{(n)} = l_{\min}$ , where  $l_{\min}$  roughly characterizes an interparticle spacing and will be defined more precisely in part 3.3.

The procedure outlined above describes the idea of a more efficient partitioning than a space-filling one, a more efficient coarsegraining of the data set because the largest voids are systematically excluded, generation by generation in  $n$ . We do not have only one partition but a hierarchy  $n = 1, 2, \dots, n_{\max}$  of partitions, each with interval sizes  $l^{(n)}$ .

A pencil and paper sketch of about sixteen points with two big voids of roughly the same size, but with three or more very nonuniform first generation clusters, e.g. figure 2, shows that the method described above will produce an efficient partition only if the clustering is relatively uniform, only if all clusters in each generation are all of about the same size. When this is not the case, when the clustering is very nonuniform (as in figure 2), then the procedure outlined above will not produce an efficient partition and may even fail to cover the set. In that case we could try to repair the misfit by taking  $l^{(n)}$  to be the largest of the intervals in the  $n$ th generation, but this may produce overlapping intervals,  $N_n l^{(n)} > 1$ , which is intolerable.

We explain in the next section how “convergence problems” arise in the analysis of empirical data whenever arbitrary (rather than efficient) partitions are used.

The motivation for the expectation that an *optimal* partition may exist, at least in *some* cases, is as follows: certain nonintegrable dynamical systems coarsegrain phase space uniquely ([21], [16]). In those systems the optimal partition is generated by the dynamics and is called the “generating partition”. As a simple example, the invariant set of the ternary tent map is the middle thirds Cantor set ([53]). The generating partition of the ternary tent map (obtained by  $n$  backward iterations of the unit interval using that map) is given by  $N_n = 2^n$  intervals  $l^{(n)} = 3^{-n}$ , for  $n = 1, 2, \dots$ . It is impossible to construct a more efficient coarsegraining of the middle thirds Cantor set than this one. The voids are the excluded open intervals  $(1/3, 2/3)$ ,  $(1/9, 2/9)$ ,  $(7/9, 8/9)$ , and so on (initial conditions of the ternary tent map that lie in the voids iterate to minus infinity).

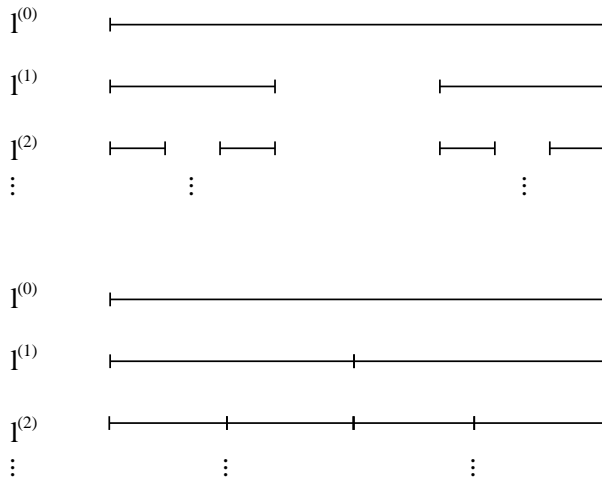


Figure 3: On top we show the optimal partitioning for the middle–thirds Cantor set, on the bottom a very inefficient uniform partitioning.

### 3.2 Scale invariant clustering

We restrict our considerations in this section to relatively uniform clustering (the clusters in a generation  $n$  of coarsegraining are all of about the same size  $l^{(n)}$ , and the  $n$ th generation voids are also all of about the same size  $v_n$ ). Invariant quantities (scaling exponents) can only be constructed, if at all, from  $N_n$  and  $l^{(n)}$  as the generation  $n$  of coarsegraining is increased, as we look at the data set with finer and finer, but *never* with *pointwise* resolution (the smallest interval size  $l_{\min}$  always contains at least *two* data points).

In what follows it is conceptually useful to think of the hierarchy of intervals for  $n = 1, 2, \dots, n_{\max}$  as sitting on the branches of a tree of some order  $t$ . There are  $N_1$  branches in generation 1,  $N_2$  in generation 2, and so on, and the tree need not be complete. Scale invariance will be seen below to require that  $N_n$  increases exponentially,  $N_n \approx t^n$ , as  $l^{(n)}$  decreases exponentially,  $l^{(n)} \approx a^{-n}$ . Complete trees have  $N_n = t^n$  branches in generation  $n$  with  $t \geq 2$  an integer, while incomplete ones have noninteger  $t$ , in which case the order of the tree is the next integer larger than  $t$ . The middle thirds Cantor set, an idealized model of uniform clustering exhibiting big voids on all scales, defines a complete binary tree ( $t = 2$ ).

We are only treating coarsegrained versions of  $N$  points, so the simplest kind of scale invariance is geometric (and so is the more complicated kind, as we shall see in parts 3.4 and 3.6 below). A fine-grained picture of the subset of any branch for  $n \geq 2$  looks, upon magnification, like the entire tree. This kind of scale invariance ([42]) is expressed by the exponent  $D_0$  in

$$N_n \left( l^{(n)} \right)^{D_0} \approx 1. \quad (1)$$

In other words,  $D_0 \approx \ln(t)/\ln(a)$  is an exponent that reflects self–similarity of a hierarchy of relatively *uniform* clusters (clusters within clusters within ...).

In order to check whether (1) holds approximately for a given (very uniform) data set it is very useful first to find as efficient a partition as possible. The practical difference (emphasizing the famous “convergence” problem) between the use of efficient and inefficient partitions is best illustrated by an idealized example.

As an example of an optimal partition consider a very artificial data set constructed as follows: arbitrarily choose a finite number  $N$  of points generated by ternary expansions of the form  $x = .\epsilon_1 \dots \epsilon_N \dots$  with  $\epsilon_i = 0$  or  $2$  ( $\epsilon_i = 1$  is excluded). These numbers belong to the middle–thirds Cantor set (all ternary numbers of this kind define the middle–thirds Cantor set [25]). Terminating strings  $\epsilon_1 \dots \epsilon_N 00000 \dots$  define  $N_n = 2^n$  intervals  $l^{(n)} = 3^{-n}$  given by  $[0, 1/3]$  and  $[2/3, 1]$  in

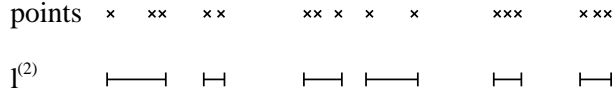


Figure 4: An efficient (nonuniform) partition  $l^{(2)}$  for the point set shown in Figure 2.

generation one ( $n = 1$ ),  $[0, 1/9]$ ,  $[2/9, 1/3]$ ,  $[2/3, 7/9]$ , and  $[8/9, 1]$  for  $n = 2$ , and so on. Rational numbers of the form  $x = .\epsilon_1\epsilon_2 \dots \epsilon_N$  (periodic expansions like  $x = .020202 \dots$ ) and irrational ones  $x = .\epsilon_1 \dots \epsilon_N \dots$  (where the digit string is nonperiodic) are also covered by all of the  $N_n$  intervals as well, so that the covering provided by those  $N_n$  intervals  $l^{(n)} = 3^{-n}$  is optimal, generation by generation. The scaling law (1) yields  $D_0 = \ln 2 / \ln 3$ . This example illustrates a “monofractal” because the optimal covering is uniform (all  $N_n$  of the optimal intervals in one generation have the same size  $l^{(n)}$ ).

In contrast, we can try to estimate  $D_0$  by using the uniform nonoptimal covering  $l^{(n)} = 2^{-n}$ , a space-filling partition given by  $[0, 1/2]$  and  $[1/2, 1]$  for  $n = 1$ ,  $[0, 1/4]$ ,  $[1/4, 1/2]$ ,  $[1/2, 3/4]$ , and  $[3/4, 1]$  for  $n = 2$ , etc., that ignores the voids altogether. Here, with  $N$  points in the data set  $N \gg N_n \gg 1$  must be very large before we can expect to observe scaling with an exponent close to  $D_0 = \ln 2 / \ln 3$ : for  $N = 16$  points, e.g., and using  $N_n \approx l^{-D}$  then from  $n = 1$  and 2 one gets  $D = 1$ ,  $n = 3$  yields  $D = .86$ , and further attempts to extract  $D_0$  are impossible unless the number  $N$  of data points is increased. This illustrates why, in practice only relatively efficient partitions are of interest. We return next to the search for the optimal partition of a typically nonuniform empirical data set of  $N$  points.

### 3.3 The optimal partition of an empirical data set

For a typical empirical data set of  $N$  points the most efficient partition that one can construct will rarely be uniform. Let  $l^{(n)}$  denote the size of the largest cluster in generation  $n$  after deleting the largest voids, as in part 3.1. This may yield an overlapping partition of  $N_n$  uniform intervals  $l^{(n)}$  where  $N_n l^{(n)} > 1$ , but we can immediately improve upon that coarsegraining: in any generation  $n$  the  $N_n$  intervals so-constructed will (excepting the largest interval, which determines  $l^{(n)}$ ) not end on data points but will extend beyond them. To make the covering efficient simply shrink each interval until it ends on the nearest two points of the cluster that it was intended to cover in the first place. The result is that the number of intervals is exactly the same as before, but we now have  $N_n$  nonuniform intervals obeying both  $l_1 + \dots + l_{N_n} < 1$  and  $l_1 \dots l_{N_n} < N_n l^{(n)}$ . In other words, we have minimized the sum  $l_1 + \dots + l_{N_n}$  while holding  $N_n$  fixed. It is hard to see how a more efficient covering can be found, so for the purpose of this paper we call the hierarchy of intervals, so-constructed, the optimal partition (see Figure 4).

Our definition of optimal partition is a finite precision realization of an “optimal”  $\delta$ -covering (a  $\delta$ -covering approximates the “infimum”), as is used in the mathematicians’ definition of “Hausdorff measure” ([19]). The method in the cosmology literature that may come nearest to ours, in spirit, is the minimal spanning tree method ([74]). In dynamical systems theory the optimal partition is called the generating partition and provides the geometric or finite precision, definition of a fractal.

Here’s an idealized example of a dynamical system with a nonuniform optimal partition ([53]). The generating partition of the asymmetric tent map with slope magnitudes  $a$  and  $b$  is given by  $N_n = 2^n$  intervals  $l_m = a^{-m} b^{-(n-m)}$  where  $m = 0, 1, 2, \dots, n$ , and describes the two-scale Cantor set (there are two first generation scales  $l_1 = a^{-1}$  and  $l_2 = b^{-1}$ ). The idealized data set consists of interval end points and also of limits of infinite sequences of interval end points (the latter corresponding to infinitely-many backward iterations of the unit interval by the asymmetric tent map). This description of the asymmetric tent map is correct if  $a^{-1} + b^{-1} \leq 1$  ( $a^{-1} + b^{-1} = 1$  means space-filling, while  $a^{-1} + b^{-1} < 1$  produces voids and clustering, representing an idealized nonuniform “Cantor dust” ([42]). One object of [16] was to extract the generating partition of the

Henon map.

The generalization of the scaling law (1) to our hierarchy of nonuniform optimal partitions  $\{l_i\}$  is

$$\sum_{i=1}^{N_N} l_i^{D_H} \approx 1, \quad (2)$$

where the scaling index  $D_H$  is called the Hausdorff dimension ([19]). Whether a data set has a Hausdorff dimension can only be answered empirically, by constructing the optimal partition and checking to see whether (2) holds over many different generations  $n$  with the same exponent  $D_H$ .

The Hausdorff dimension of the two-scale Cantor set is given exactly in the first generation by  $a^{-D_H} + b^{-D_H} = 1$ . In the empirical case, in contrast,  $N \gg N_n \gg 1$  is usually required in order that we have enough data points to see scaling via either (1) or (2) which, as Mandelbrot [42] pointed out early in his book, is usually confined to an intermediate range of interval sizes  $l^{(n)}$  where  $l_{\max} \gg l^{(n)} \gg l_{\min}$ . Here,  $l_{\max}$  is on the order of the size of the sample,  $l^{(n)}$  is the largest of the  $N_n$   $n$ th generation intervals  $\{l_i\}$ , and  $l_{\min}$  is in our case the smallest distance between two points in the sample. In general, we should not expect to observe scaling unless the largest intervals are much smaller than the size of the system, and unless all of the smallest ones contain more than a single data point. However, the larger limit may not be applicable to present astronomical data because the systems of galactic clusters and voids are presumably much larger than any available sample size. Also, there is nothing to prevent our checking for scaling all the way down to  $l_{\min}$ . Again, if an inefficient partition is chosen then scaling may not be observed even if the data set is fractal, because the number  $n$  of generations needed for “convergence” to a scaling exponent  $D_0$  or  $D_H$  may exceed the number  $N$  of data points in the sample.

*All definitions and approximations based upon the  $l^{(n)} \rightarrow 0$  limit are systematically avoided because, as we explain below, they lead to formulae that generally do not apply to finite data sets.*

Suppose that we have found the optimal nonuniform partition for a data set. If we replace the uneven intervals in a nonuniform partition  $\{l_i\}$  by the largest scale of each generation (simply call it  $l^{(n)}$ ), then we obtain a less optimal uniform covering defined by

$$N_n \left( l^{(n)} \right)^{D_0} \approx 1. \quad (3)$$

Because  $N_n$  is the same as in (2), and because  $l^{(n)} \geq l_i$ , it follows that  $D_0 \geq D_H$  where  $D_0$  is called the box-counting dimension. This procedure defines the most efficient *uniform* partitioning of the data set if the clustering is relatively uniform. In other words, whether or not  $D_0$  provides a good estimate of  $D_H$  for low values of  $n \ll N$  depends on whether or not the uniform partition closely approximates the nonuniform optimal one. This replacement amounts to the pointwise approximation of a nonuniform fractal data set by a monofractal. The resulting idealized data set can be thought of as consisting of the end points of the uniform intervals  $l^{(n)}$ . For the two-scale Cantor set with  $a < b$  the box-counting dimension is  $D_0 = \ln 2 / \ln a$ . In the two-scale Cantor set  $D_0 = \ln 2 / \ln a$  and  $a^{-D_H} + b^{-D_H} = 1$  yield  $D_0 \approx D_H$  only if  $a$  and  $b$  are approximately equal.

How many generations are necessary in order to convince hardened sceptics that scaling has been observed? In both critical phenomena and dynamical systems theory the rule of thumb is three decades on a log-log plot, requiring astronomical data, e.g., from .1 to 100  $h^{-1}$ Mpc, or from 1 to 1000  $h^{-1}$ Mpc depending on the smallest distance reported in a given catalog of galaxies. With  $l^{(n)} \approx a^{-n}$ ,  $a \geq 2$ , we would need  $n \approx 3 \ln 10 / \ln a$  generations. We call this criterion “the Geilo Criterion” because it was suggested at a Geilo NATO-ASI. The Geilo criterion is not a matter of taste: it is advocated in order to deflect erroneous reports of scaling like that indicated in figure 1 over only two decades,  $1 \leq r \leq 100$ .

Thinking of the optimal partition of a fractal as organized onto a tree of some order, if we write  $N_n = t^n$  then the order of the tree is the next integer greater than or equal to  $t$ . If  $t$  is nonintegral then the tree is incomplete. If  $l^{(n)} = a^{-n}$  then  $t = a^{D_0}$ . With  $a \geq 2$  the  $\beta$ -model of fluid turbulence lies on an incomplete tree that is at least octal ([51]). See [11] for a discussion of the  $\beta$ -model in cosmology.



### 3.4 Multifractal scaling (via a nonuniform optimal partition)

A data set that obeys scaling (2) with a nonuniform optimal partition may be “multifractal”. Multifractal is always defined here to mean a spectrum of fractal dimensions ([30]). Each dimension in a multifractal spectrum describes the scaling of a subset of the optimal partition (a nonuniform fractal is decomposed disjointly into a union of other fractals).

Given the optimal partition a multifractal spectrum  $D(\lambda)$  may be defined by parameterizing the hierarchy of coarsegrained intervals (the parameter here is  $\lambda$ ) so that the partition is organized into (nonoverlapping but) interwoven sub-partitions ([65]). Each fractal dimension in the multifractal spectrum is the Hausdorff dimension of one subset of the partition (a multifractal is always the union of a complete set of nonoverlapping but interwoven fractals labeled systematically by some index). To obtain scale invariance the interval sizes  $l_n$  must contract exponentially as  $n$  increases. Both the  $n$ th generation intervals and their contraction rates are generally nonuniform: as an oversimplified example let  $l_i = a_i^{-n}$  denote the  $i$ th of  $N_n$  intervals in generation  $n$ . This defines a simple nonuniform Cantor set based on  $N_1$  different first generation scales  $l_i = a_i^{-1} = e^{-\lambda_i}$  if  $l_1 + \dots + l_{N_1} < 1$  (in a chaotic dynamical system the contraction rate  $l_i^{(n)} \approx e^{-n\lambda_i}$  describes the intervals of the generating partition only asymptotically and approximately for  $n \gg 1$ , representing the inverse butterfly effect for integration backward in time along unstable manifolds ([53])).

Suppose that there are  $N(\lambda)$  intervals with the same contraction exponent  $\lambda$  (in a dynamical system  $\lambda_i$  is the Liapunov exponent for forward evolution in time, starting from a specific class of initial conditions, namely, all initial conditions that yield the same Liapunov exponent  $\lambda_i$ ). Then  $N(\lambda) = l(\lambda)^{-D(\lambda)}$  (where  $l(\lambda) = e^{-\lambda}$ ) defines the Hausdorff dimension  $D(\lambda)$  of the subset of the partition labeled by  $\lambda$ . We can generalize (2) by writing down the generating function ([65])

$$Z_n(\beta) = \sum_{i=1}^{N_n} l_i^\beta = \sum_{\lambda} N(\lambda) l(\lambda)^\beta \approx \sum_{\lambda} e^{s(\lambda) - \beta\lambda} \quad (4)$$

with  $N(l) \approx e^{ns(\lambda)}$  for large enough  $n$ , and where  $Z_n(D_H) \approx 1$  defines the Hausdorff dimension of the entire fractal (by (2)). Note that  $D_H > D(\lambda)$  because  $N(\lambda) < N_n$ . This simple fractal, seen as multifractal, is the union of a complete set of interwoven, nonoverlapping monofractals (neighboring branches on each generation of the tree generally are labeled by different indices  $\lambda$ ). In the oversimplified model above we have  $Z_n(\beta) = \left(\sum a_i^{-\beta}\right)^n$ .

As an example ([53]), consider the two scale Cantor set (with  $N_1 = 2$  first generation intervals  $l_1 = a^{-1} > l_2 = b^{-1}$ ). In generation  $n$  the optimal covering is given by the  $N_n = 2^n$  intervals with sizes  $l_1^m l_2^{n-m}$ , of which  $N_m = n!/m!(n-m)!$  have the same size  $l_m = l_1^m l_2^{n-m}$ . Here,  $\lambda = x \ln a + (1-x) \ln b$  with  $x = m/n = 0, 1/n, \dots, 1$ . In each generation  $n$  there are  $n+1$  points in the multifractal spectrum, not more, and the number of points grows only linearly with  $n$  (still, this eliminates bi-fractals, tri-fractals,  $\dots$ , and  $N$ -fractals from our definition of “multifractal”). Using Stirling’s approximation, so that, with  $x = m/n$ ,  $N(\lambda) \approx e^{ns(\lambda)}$  where

$$s(\lambda) \approx -x \ln x - (1-x) \ln(1-x) \quad (5)$$

is the Boltzmann entropy (divided by  $n$ ) of all intervals with the same contraction exponent  $\lambda$ , we have  $D(\lambda) = s(\lambda)/\lambda$ , which shows the connection of fractal dimension to entropy ( $s(\lambda) = \ln 2$  and  $\lambda = \ln 3$  for the middle thirds Cantor set). Since  $t(\lambda) = e^{s(\lambda)}$  the tree is generally binary but incomplete for any monofractal subset labeled by the contraction index  $\lambda$  in the two-scale Cantor set.

Note that “multifractal” is consistent with  $D_H = 1$ : the support may be space-filling, while subsets of the support are fractal ( $0 < D(\lambda) < 1$ ). In the two-scale Cantor set  $D_H = 1$  corresponds to the space-filling condition  $a^{-1} + b^{-1} = 1$ .

Ideas based on the generating function (4) have been used to analyze experiments on the transition to chaos in fluid dynamics ([26]).

The notion that multifractal scaling can be verified for small data sets ([48]) is a misconception: fewer data points  $N$ , with less precision, *cannot* be required for the determination of a *spectrum*

of fractal dimensions than are required for determining *one* dimension, say  $D_H$ . The error in the claim follows from confusion and errors made in defining “multifractal” (see parts 4, 6 and 7 below).

The term multifractal has occasionally been incorrectly defined in the cosmology literature where at least three entirely different generating functions are confused together (see parts 4 and 6) as if their corresponding scaling exponents (whenever scaling exists) would define universality classes independently of probability distributions and partitionings used to define those exponents. In [13] a far too restrictive idea of multifractal is presented in part 6. Multifractal spectra were introduced in analogy with critical exponents ([30]), but the expectation of universality ([39]) was not realized (a restricted and still unproven universality is merely postulated for vortex cascades in fluid turbulence ([24])). In the theory of chaotic dynamical systems two examples of topologic invariants are the tree order  $t$  and its degree of incompleteness ([28], [53]).

We always restrict our formulation of the requirement for fractal and multifractal scaling to finite  $l^{(n)}$  and to finitely many data points  $N$ , completely avoiding mathematically idealized results that would require for their applicability the empirically and computationally unattainable limit where  $l^{(n)} \rightarrow 0$ . We shall see in part 3.6 that this rules out largest term approximations, whose validity would require values of  $l^{(n)}$  that are too much small ( $l^{(n)} \ll 1$ , with the range of  $l^{(n)}$  extending over at least three decades) to be consistent with the analysis of galaxy distributions.

### 3.5 The empirical distribution

For an observational data set there is only one pointwise probability distribution, the empirical distribution  $P(x)$  defined by the  $N$  data points:  $P(x)$  is simply the fraction of points lying to the left of (and including)  $x$ , so that  $P(0) = 1/N$  and  $P(1) = 1$ , by construction. The distribution is constant on the voids and increases discontinuously at each data point, so that the plot of  $P(x)$  is a staircase of  $N - 2$  steps of finite width. The data staircase has the singular pointwise density  $\rho(x) = P'(x)$  given by

$$dP(x) = \frac{dx}{N} \sum_{i=1}^N \delta(x - x_i) \quad (6)$$

Of course, (6) is only a theorist’s fiction: it neglects the error bars in the locations of positions. In reality each position is specified empirically by a finite *interval* whose width is the uncertainty in location. We assume here that these uncertainties are very small relative to the smallest separation  $l_{\min}$  between data points. Otherwise coarsegraining and fractal/multifractal analysis are impossible. The density (6) will be used to correct a more serious theoretical error in part 6 below.

All that we need in what follows is the staircase  $P(x)$  along with an empirical technique for characterizing voids and clusters. We emphasize that attempts to “smooth” the staircase (via “splines”, e.g) will discard important information about clustering. *No pointwise probability distribution other than the staircase  $P(x)$ ,*

$$P(x) = \frac{1}{N} \sum_{i=1}^N \Theta(x - x_i) \quad (7)$$

*is relevant for empirical data analysis.*

An arbitrary distribution  $P(x)$  of  $N$  data points is generally not approximable in either the continuum (infinite precision) or hydrodynamic (coarsegrained) limit by a differentiable distribution. We shall find next that the coarsegrained versions of the empirical distribution  $P(x)$  are typically too spiky (too intermittent) to be approximable by an everywhere differentiable distribution (reminding us more of “noise” than of analyticity), even if  $D_H$  is an integer (even if the optimal partition is space-filling). The spikiness/intermittence represent clustering and voids in the sample. Hydrodynamics demands a coarsegrained description of a pointwise distribution, and we will discuss in part 8 how the required densities can be defined.

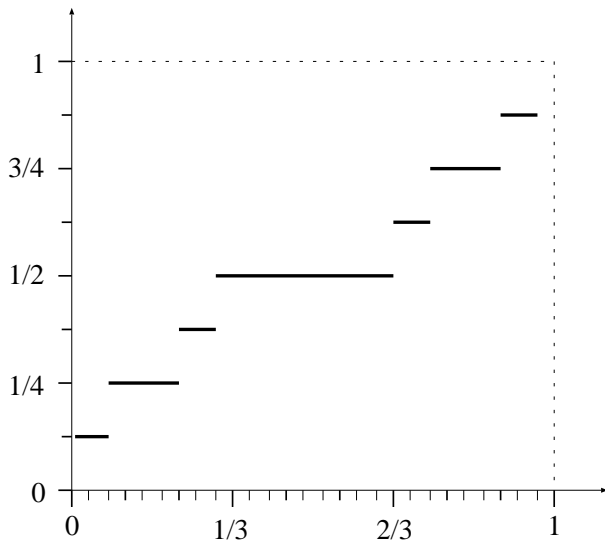


Figure 5: The idealized empirical distribution according to eq. 8 with  $N = 3$ .

On an optimal or at least efficient partition a coarsegrained probability  $P_i$  is defined by the difference  $P_i = \Delta P(x)$  over the  $i$ th closed interval of size  $l^{(n)}$ , and is just the fraction  $P_i = n_i/N$  of the total number of data points  $n_i$  in the  $i$ th interval including the end points. While each empirical distribution  $P(x)$  is a staircase of finitely-many steps, each coarsegrained distribution  $\{P_i\}$  is a histogram on a finite support.

The optimal partition optimally defines the “support” of the hierarchy of coarsegrained empirical distributions  $\{P_i\}$ : for the optimal partition, each interval end point coincides with a point where the staircase function  $P(x)$  increases discontinuously. Whether an empirically-constructed optimal partition is the generating partition of a deterministic dynamical system is a separate question (the main question, but very hard to answer ([16], [26])).

The coarsegrained probabilities  $\{P_i\}$  can be used to perform averages that ignore the details of the dynamics at all scales smaller than  $l^{(n)}$  (coarsegraining the smaller scales is required in order to define hydrodynamics). The only limitation, so far, is that  $1/2 \geq l^{(n)} \geq l_{\min}$ . Bear in mind however, that before reaching the smallest scale  $l_{\min}$ , as  $n$  is increased, we may not be able to distinguish clustering from voids without ambiguity. Even if clustering and voids are present at all scales they may not be scale invariant. The construction of efficient and even optimal partitions does not presume scale invariance, rather, the converse is true, especially in practice.

We have used the frequency definition of probabilities because it arises naturally in both empirical data analysis and computer simulations. Using our simple example above, however, we can offer as an idealized staircase distribution the Cantor function ([25], [53])

$$P(x) = .\frac{\epsilon_1}{2} \frac{\epsilon_2}{2} \dots \frac{\epsilon_N}{2} \dots, \quad (8)$$

where, because  $x = .\epsilon_1\epsilon_2\dots\epsilon_N\dots$  is a ternary number with  $\epsilon_i = 0$  or  $2$ ,  $P(x)$  is a binary number (because  $\epsilon_i/2 = 0$  or  $1$ ). This staircase describes a mathematician’s idealization of empirical data, namely, one (of infinitely-many) distribution that can be constructed by using points in the middle-thirds Cantor set:  $P(0) = 0$ ,  $P(1) = 1$ ,  $P(x)$  is constant on the open voids and increases discontinuously at the end point of any closed interval  $l^{(n)} = 3^{-n}$  of the optimal covering, where the change in  $P(x)$  is  $\Delta P = 2^{-n}$ . Therefore, the Cantor function defines a hierarchy of *uniform* coarsegrained distributions  $P_i = \Delta P(x) = N_n^{-1} = 2^{-n}$ , generation by generation in  $n$ , on the fractal support  $l^{(n)} = 3^{-n}$ . The plot of the Cantor function, the mathematicians’ idealization of an empirical distribution, is called a *devil’s staircase* because it has  $2^\infty$  steps.

A good way to look for voids is simply to plot the empirical staircase:  $P(x)$  is constant on the voids, where there are no data points. This is illustrated by the idealized example described above (see also figure 5). Unfortunately this method is not trivially generalizable to more than one dimensions.

The Cantor distribution reflects statistical independence based upon the two first generation probabilities  $p_1 = p_2 = 1/2$  for occupying the two first generation intervals, each of length  $l^{(1)} = 1/3$ , and is generated by the ternary tent map for a special class of initial conditions. For other initial conditions the map yields other distributions. Nonuniform distributions that lack statistical independence are trivially easy to construct via either the ternary Bernoulli shift or the ternary tent map. For example, iterate the (ternary) initial condition  $x_0 = .202002000200002\dots$ . Statistically independent distributions where  $p_1 > p_2$  can also be constructed with only a bit more effort (see ch. 9 of [53] for the method).

Summarizing, in the beginning there is only a collection of  $N$  points (or a time series) generated by some generally unknown dynamical system. We can construct the empirical distribution  $P(x)$  immediately, but we cannot construct the coarsegrained distributions  $\{P_i\}$  without first extracting the optimal partition  $\{I_i\}$ . In dynamical systems theory the optimal partition is provided by the generating partition. The generating partition, if it exists, is the signature of the dynamical system because it shows how the dynamics coarsegrains phase space naturally. In contrast, the histograms that appear on the optimal support can be produced by every system in the same topologic universality class (symbolic dynamics is universal for all systems in the same universality class ([28], [53])), so that a particular statistical distribution  $\{P_i\}$  cannot be the signature of a particular dynamical system. Both the Henon map and the logistic map  $f(x) = Dx(1-x)$ , with  $D_c < D < 4$ , where  $D_c$  is the period doubling critical point, belong to the same topologic universality class (both the logistic map with  $D > 4$  and the binary tent map belong to a separate universality class). Both systems, although of different spatial dimension, generate the same range of histograms (for corresponding classes of initial conditions), but on different supports. From the perspective of both dynamical systems theory and the search for scale invariance the central problem of data analysis is to extract the optimal partition of a particular set of data points. See ref. [26] and [56] for examples of the extraction of optimal partitions from data in fluid mechanics.

### 3.6 Multifractal scaling (via the empirical distribution $P(x)$ on an efficient support)

A nonuniform distribution on a fractal support looks fractally-fragmented (looks more and more spiky as the support is viewed with finer and finer resolution  $l^{(n)}$ ). Distributions on space-filling supports may also be fractally fragmented, as we shall see below. A nonuniform distribution on a uniform or nonuniform support (that is either fractal or space-filling) can be used to sort and label fractal subsets of the support. Each subset has its own fractal dimension  $d(\alpha)$ , where  $\alpha$  is the labeling-index [30]. Multifractal, in this paper, always means a spectrum of fractal dimensions, where each dimension describes the scaling via (1) or (2) of a subset of the support of  $P(x)$ . We will show in parts 6 and 7 why the attempt to use other definitions leads to confusion and failed expectations (predictions of “dimensions” that are not the dimension of anything are discussed in parts 4 and 6).

First, note that for a uniform distribution on a uniform support we can write  $P_i = N_n^{-1} = (l^{(n)})^{D_0}$ . To describe a nonuniform distribution on a uniform or nonuniform support in generation  $n$  of coarsegraining, we try to define scaling exponents  $\alpha_i$  by writing  $P_i = l_i^{\alpha_i}$ , where the scaling index  $\alpha_i$  takes on the same value  $\alpha_i = \alpha$  on  $N(\alpha)$  different intervals which we denote (using very sloppy but obvious notation) by  $l_1, \dots, l_{N(\alpha)}$ . Therefore, by (2), we can write

$$\sum_{i=1}^{N(\alpha)} l_i^{d(\alpha)} \approx 1 \quad (9)$$

to define  $d(\alpha)$  as the Hausdorff dimension of the subset of the support where  $\alpha_i = \alpha$  (if, indeed, such scaling holds). If we could accurately replace the optimal nonuniform partition by the largest term

$l(\alpha) = \max\{l_i : i = 1, \dots, N(\alpha)\}$  in the subset, then we would obtain  $N(\alpha) = l(\alpha)^{-f(\alpha)}$ , where  $D_H > f(\alpha) > d(\alpha)$ . In other words,  $f(\alpha)$  is the box-counting dimension for  $N(\alpha)$  nonoverlapping uniform intervals of size  $l(\alpha)$ . This replacement works only for relatively uniform sub-clustering. Otherwise it is necessary to compute  $d(\alpha)$ .

Given a nonuniform empirical distribution  $P(x)$  over an optimal uniform partition, whether or not the histograms  $\{P_i\}$  scale over a reasonable range of different sizes of  $l_i$ ,  $P_i = l^{\alpha_i}$ , is the main question for empirical data analysis. In cosmology  $P_i = n_i/N$  is the fraction (out of a total number  $N$  of galaxies) of galaxies in the  $i$ th interval  $l_i$ .

In all data analysis and computer simulations there can be at most finitely many values of  $\alpha$  and  $f(\alpha)$  (and finitely-many values of  $\lambda$  and  $D(\lambda)$  as well) because  $N_n \ll N$  is finite ( $N \approx 400$  for typical galaxy samples). However, the number of points in a spectrum will grow generation by generation  $n$  for a multifractal spectrum (again, this distinguishes multifractal from bi-fractal, tri-fractal,  $\dots$ ,  $N$ -fractal) within the cutoff limits  $l_{\max} \geq l^{(n)} \geq l_{\min}$ . We can illustrate this via a simple example of an  $f(\alpha)$  spectrum, the one given by the two-scale Cantor set with first generation probabilities  $p_1 > p_2$  describing statistical independence ([30]) in all higher generations, and optimal first generation intervals  $l_1 = a^{-1}$  and  $l_2 = b^{-1}$ . In this case, fixing the scaling index  $\alpha$  picks out a monofractal, so that  $d(\alpha) = f(\alpha)$  because all intervals in the subset have the same size  $l_m = l_1^m l_2^{n-m}$ . By using Stirling's approximation on  $n!$  (requiring  $n \gg 1$ ), we then obtain, with

$$\alpha = \frac{-x \ln p_1 - (1-x) \ln p_2}{x \ln a + (1-x) \ln b}, \quad (10)$$

that

$$f(\alpha) \approx \frac{-x \ln x - (1-x) \ln(1-x)}{x \ln a + (1-x) \ln b}, \quad (11)$$

where  $x = m/n = 0, 1/n, 2/n, \dots, 1$  parameterizes both  $\alpha$  and  $f(\alpha)$ . There are  $n+1$  points in the spectrum so that  $f_{\max}(a) < D_H$ , where  $a^{-D_H} + b^{-D_H} = 1$  defines  $D_H$ . Note also that  $f(\alpha) = s(x)/\lambda(x)$ , as expected.

We can summarize our present terminology by writing down either the generating function ([30])

$$\chi_n(q) = \sum_{i=1}^{N_n} P_i^q \quad (12)$$

or the generation function ([34])

$$\Gamma_n(q) = \sum_{i=1}^{N_n} \frac{P_i^q}{l_i^q} \approx 1 \quad (13)$$

where, in the empirical search for scaling laws, it is first necessary to find an approximately *optimal partition* in order correctly to extract a multifractal spectrum of dimensions  $f(\alpha)$ , or even one fractal dimension  $D_H$ . Otherwise the convergence requirements (the number  $n$  of generations in a hierarchy  $\{l_i\}$  of interval sizes) needed to see scaling with an approximately correct exponent almost always outruns the limitation placed by the number  $N$  of points in an empirical sample.

When multifractal scaling can be shown to hold over enough different generations  $n$  of interval sizes  $l^{(n)}$ , then we can also write

$$\chi_n(q) \approx \sum_{\alpha} l(\alpha)_i^{q\alpha - f(\alpha)} \quad (14)$$

and

$$\Gamma_n(q) \approx \sum_{\alpha} l(\alpha)^{q\alpha - f(\alpha) - \tau} \approx 1. \quad (15)$$

Note that (13) generalizes (2) so that we can explicitly discuss nonuniform distributions of points on the support, as with (12).

By using  $P_i = N_n^{-1}$  in (13) we get a result that looks formally like the generating function  $Z_n(\beta)$  in (4) above if we set  $\beta = -\tau$  and  $N_n^q = Z_n(\beta)$ . Note, however, that no assumption about the

distribution of points  $\{P_i\}$  over the support  $\{l_i\}$  was necessary in order to define the generating function (4). In dynamical systems theory the generating function  $Z_n(\beta)$  can be rewritten via symbolic dynamics as the partition function for a one dimensional Ising model ([34]) with long range interactions in equilibrium statistical mechanics ( $\beta$  is then the inverse temperature).

Most discussions of multifractals inevitably stress that the generating functions (12) and (13) should *themselves* scale approximately in the limit  $l^{(n)} \rightarrow 0$  where, due to domination of the entire sum by  $N(\alpha)$  largest terms ([30], [43]), all of the same size (and parameterized by  $q$ ),

$$\chi_n(q) \approx l(\alpha)^{q\alpha(q)-f(\alpha(q))} \quad (16)$$

or

$$\Gamma_n(q) \approx l(\alpha)^{q\alpha(q)-f(\alpha(q))-\tau(q)} \approx 1 \quad (17)$$

where (because  $n$  goes to infinity as  $l^{(n)} \rightarrow 0$ ) we would hypothetically obtain an  $f(\alpha)$  curve parameterized by  $q$ . In this case, because there are enough points in the spectrum that  $f(\alpha)$  may be differentiated accurately, the “generalized dimensions”  $D_q$  can be defined by  $\tau(q) = (q-1)D_q = q\alpha(q) - f(\alpha(q))$ , where  $\alpha = \tau'(q)$  is the slope in the plot of  $\tau$  vs.  $q$  and  $q = f'(\alpha(q))$  is the slope of the  $f(\alpha)$  curve. *This continuum limit is misleading because it is generally inapplicable to data analysis.*

To see this, merely note that both generating functions are sums over all possible scales,

$$\chi_n(q) \approx l(\alpha_1)^{q\alpha_1(q)-f(\alpha_1(q))} + \dots + l(\alpha_k)^{q\alpha_k(q)-f(\alpha_k(q))} \quad (18)$$

(or, in the case of a nonuniform distribution on a monofractal, over  $N_n$  terms  $l^{\alpha_i}$  with different exponents  $\alpha_i$ ). For finite  $l^{(n)}$  the generating functions (14) and (15) *cannot* scale approximately unless  $l^{(n)}$  is small enough,  $l^{(n)} \ll \ll 1$  (we cannot emphasize this requirement too strongly), that a largest term approximation is accurate, which is generally *not* the case. Formulations and expectations of scaling based on the  $l^{(n)} \rightarrow 0$  limits (16) and (17) have been taken seriously enough to have been employed during data analysis within the cosmology community ([37]), as elsewhere. In data analysis this approximation is usually a very bad one (see Theilor [73] for a clear and comprehensive exposition of the usual assumptions made in discussions of multifractal generating functions).

In typical data analyses found in the literature the largest term approximation is implicit in any plot of the logarithm of a generating function vs.  $\ln l^{(n)}$  in the search for generalized dimensions  $D_q$ . We expect that most empirical data will not produce small enough values of  $l^{(n)}$  for a largest term approximation to be applicable. *Even if multifractal scaling should hold term by term in (12), in the form of (18), it cannot be discovered by a plot of  $\ln \chi_n$  vs.  $\ln l^{(n)}$ .* Instead, one must check for scaling term by term inside the sum (12). *In other words, forget the sums (12) and (13) and check each term separately for scaling,* to verify whether  $P_i = l_i^{\alpha_i}$  with  $N(\alpha) = l_i^{-f(\alpha)}$  actually holds over a Geilo-range of scale sizes. The generating functions are not directly measurable anyway, so one needn’t care whether or not they scale.

The coarsegrained density defined by  $\rho_i = P_i/l_i = l_i^{\alpha_i-1}$  is typically singular. Even if the support is space-filling (even if  $D_H = 1$ ) the coarsegrained density will look more and more intermittent as the resolution is improved if the distribution  $P(x)$  has nonuniform clusters that are scale invariant (see [56] for a one dimensional example from fluid turbulence). Any attempt to replace a staircase  $P(x)$  by a distribution with a differentiable density may delete, mask, or, at best, unnecessarily complicate the description of clustering and intermittence. Why introduce the mathematical fiction of a continuous distribution when observation gives us tractable discreteness directly?

## 4 The correlation integral

In cosmology ([60], [13], [6]), as it was in empirical analyses of dynamical systems ten years ago (before the partitioning ([21]) and recycling ([16]) of strange sets), it is usual to work with the

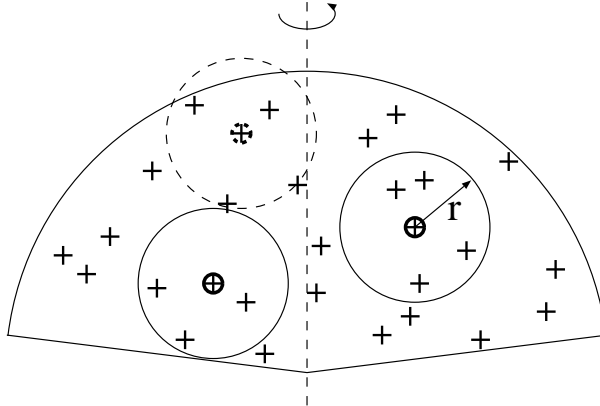


Figure 6: A sketch of the sample, illustrating which galaxies we use (solid circle) and don't use (dashed circle) in the search for scale invariance.

correlation integral

$$n(r) = \frac{1}{N} \sum_{i=1}^N n_i(r) \quad (19)$$

where “the correlation integrand”

$$n_i(r) = \frac{1}{N} \sum_{i \neq j=1}^N \theta(r - |x_i - x_j|) \quad (20)$$

is the fraction of galaxies in a sphere of radius  $r$ , centered on the  $i$ th of  $N$  galaxies. Here, we take  $0 < r < 1$ . This means that the original dimensional variable  $r$  for each galaxy has been rescaled by dividing it by  $r_{\max,i}$ , where  $r_{\max,i}$  is the value of the unscaled variable  $r$  for which the sphere of radius  $r$ , centered on galaxy  $i$  just touches the boundary of the data set. In other words, spheres of every radius  $r$  lie *completely* within the boundaries of the data (see figure 6). We stress that data sets should not be “extended” by adding points beyond the boundaries of the observational data during box-counting. To do so would change the data set from the one that we set out to analyze. In other words, we agree with the Pietronero school [13], but in part 5 we will show how to refine the data analysis to eliminate a certain (self-) inconsistency in that work.

Whenever the distribution in (20) exhibits statistical independence then  $n(r) = \chi_n(2)$  holds as well, as is implicit in standard treatments. Clearly, data that are statistically independent on an *optimal* partition (like the Cantor function differences  $P_i = 2^{-n}$  over the closed intervals  $I^{(n)} = 3^{-n}$ ) will not show statistical independence over an *arbitrary* partition. In the limit of small length scales the generalized dimension  $D_2$  coincides with the correlation integral dimension  $\nu$  for the case of an empirical distribution  $P(x)$  that exhibits statistical independence on its optimal coarsegrained support ([31]), but we cannot merely assume statistical independence of observational data, and the zero length limit is anyway physically unattainable. Therefore we do not expect to extract  $D_2$  via data analysis. Loosely speaking, however, one can refer to  $\nu$  as the “correlation dimension”. Note that  $\nu < 3$  requires either a multifractal distribution on a fractal support, or, for a nearly uniform distribution, the support must be fractal.

The generalization of (19) is given by the (not directly measurable) generating function

$$G_n(q) = \frac{1}{N} \sum_{i=1}^N n_i(r)^{q-1} \quad (21)$$

As in (19),  $N$  is not the number of intervals in a nonoverlapping efficient partition, but is the number of points in the data sample. *The correlation integral was first emphasized in the literature*

because it appears to allow us to circumvent the need to find an optimal partitioning. We will return to this point shortly.

Our first main point is that whether one uses (12), (13) or (21) to study galaxy counts is irrelevant: a generating function cannot scale unless all terms in the sum scale separately, and only then if one term dominates. If scaling holds locally but the data set is not monofractal, then each term in the correlation integral (19) must have the form

$$n_i(r) \approx r^{\nu(i)} \quad (22)$$

where  $\nu(i)$  is the local correlation integral index, the scaling exponent (formally somewhat analogous to  $\alpha_i$  in equation (14), except that here there is no accurate way to define a spectrum of fractal dimensions  $f(\nu)$  because an efficient partition is not defined by (21)) for galaxy counts for  $n = 1, 2, \dots, n_{\max}$  spheres with corresponding radii  $r$  centered on galaxy  $i$ . Clearly, in the absence of largest term dominance the correlation integral representing local scaling with  $N$  different indices  $\nu(i)$ ,

$$n(r) = \frac{1}{N} \sum_{i \neq j=1}^N c_i r^{\nu(i)}, \quad (23)$$

is not scale invariant because each term in the sum scales differently:  $(\lambda r)^{\nu(i)} = \lambda^{\nu(i)} r^{\nu(i)}$ . If, in a plot of  $\log n(r)$  vs.  $\log r$ , linearity is reported for a large enough range of values of  $r$  that the result is not spurious (see Figure 1, then the likelihood is that all terms inside the sum have approximately the same scaling exponent  $\nu(i) \approx \nu$ , indicating that the data set is approximately monofractal. For example, with  $N$  points distributed uniformly over the  $N_n = 2^n$  intervals of the optimal partition  $l^{(n)} = 3^{-n}$  of the middle thirds Cantor set, the correlation integral is dominated by a single term

$$n(r) = n_i(r) = 2^{-n} - 2^{-N} \quad (24)$$

and scales when  $N \gg n$ ,  $n(r) \approx 2^{-n} = r^{D_0}$  where  $D_0 = \ln 2 / \ln 3$  because  $r = 3^{-n}$ . In other words,  $n(r)$  is approximately scale invariant for  $N \gg n$  because every term  $n_i(r)$  in the sum (19) is the same and is also scale invariant. Here,  $D_0 = D_2 = \nu$  holds because we have (implicitly chosen to use) a uniform distribution on a monofractal. In particular the analysis of part 5 shows, that one cannot assume that  $n_i(r) = r^\nu + \delta n_i(r)$ , where  $\delta n_i(r)$  is Poisson noise.

In the analysis of empirical data, on the other hand, if scaling of (21) is reported but has only been observed over a non-Geilo range of values of  $r$  then the resulting spectrum of generalized correlation dimensions  $\nu_q$  in  $t(q) = (q-1)\nu_q$  defined by

$$G_n(q) = \frac{1}{N} \sum_{i=1}^N n_i(r)^{q-1} \approx r^{t(q)} \quad (25)$$

may be spurious (and appears only in the unphysical limits where  $N \rightarrow \infty$  and  $r \rightarrow 0$ ). The variation of  $t(q)$  with  $q$  obtained from a plot of  $\ln G_n(q)$  vs.  $\ln r$  over an inadequate range of  $r$ -values probably indicates that the generating function (21) does *not* scale. In [2] it is shown how one can even get a spurious “generalized dimension” spectrum from log-log plots of a *Gaussian* distribution.

We point out next that the hope that one could circumvent the need to extract the optimal partition from the empirical data was an illusion: the generating function (21) cannot be used to compute either a Hausdorff or box-counting dimension. Setting  $q = 0$  in (25), the standard approach would lead the expectation that  $\nu_0$  in

$$G_n(0) = \frac{1}{N} \sum_{i=1}^N n_i(r)^{-1} \approx r^{-\nu_0} \quad (26)$$

provides an estimate for the box counting dimension  $D_0$ . This is impossible, because neither the box counting nor information dimension is included in the  $\nu_q$  spectrum (appeals to the limit of



vanishing  $r$  ([67]) do not help in the empirical case). The reason is simple: the terms on the left hand side of (26) don't define an efficient, nonoverlapping partition of  $G_n(0)$  intervals, each of size  $r$ . Hence, the ‘‘convergence’’ difficulties reported by [48] in the attempt to estimate the box counting dimension by computing  $\nu_0$ .

If we would try instead to define an interval  $r_i$  by formally writing  $r^{\nu_0}(n_i(r)^{-1}) = r_i^d$  in (26), then the result

$$\frac{1}{N} \sum_{i=1}^N r_i^d \approx 1 \quad (27)$$

reminds us superficially of equation (2) above, but  $d$  does not define a Hausdorff dimension: the  $N$  intervals  $r_i$  overlap very badly with each other because the sum is over all  $N$  galaxies instead of over an efficient nonoverlapping partition. Equation (27) was proposed by Martinez ([45]) as one that yields  $D_H$ , as well as the  $D_q$  spectrum for  $q < 1$  via the generalization (see also [44])

$$W_n(t) = \frac{1}{N} \sum_{i=1}^N r_i^{-t} \approx p^{-q} \quad (28)$$

but information about the spectrum  $D_q$ , aside from an estimate of  $D_2$ , is not included in these formulae.

Equation (27) is supposed to be based on the equation

$$\frac{1}{N} \sum_{i=1}^N r_i \approx \overline{r_N} \quad (29)$$

with

$$\overline{r_N} \approx K N^{-1/D} \quad (30)$$

discussed by [3], where  $r_i$  is the nearest neighbor distance between two points in a sample consisting of  $N$  points. However, (29) is not the same as (27) because the partitioning in (29) is *nonoverlapping*: each point is connected only to one other point. For any finite subset of the middle-thirds Cantor set consisting only of end points, we find that  $K^{-1} = 2$  because the number of end points  $N = 2^{n+1}$  is simply twice the number of intervals  $N_n = 2^n$  required to cover those points. In this case the required nearest neighbor intervals are simply the usual nonoverlapping intervals  $r_i = 3^{-n}$  of the middle-thirds Cantor set. Notice also that one cannot stray far from the optimal result  $l^{(n)} = 3^{-n}$  by using nonterminating ternary expansions  $x = .\epsilon_1 \dots \epsilon_N \dots$  with  $\epsilon_i = 0$  or  $2$  to generate  $N$  points of the middle-thirds Cantor set rather than by using only terminating ternary strings. While scaling holds *exactly* when we use nearest neighbor distances in (29) and (30) for the mathematical idealization of a Cantor set, we should not expect an analogous ‘‘convergence rate’’ when we use empirical data. Equations (29) and (30) should only be expected to yield an accurate scaling index  $D \approx D_H$  when the nearest neighbor distances are taken to be the end points of an optimal partition.

The expectation ([47], [45]) that different generating functions can be used to compute ‘‘the  $D_q$  spectrum’’ for different ranges of  $q$ , even in the idealized limit where  $l^{(n)} \rightarrow 0$ , is based on three unfulfilled expectations. First, the box counting dimension does not belong to the  $\nu_q$  spectrum (neither does the information dimension). Second, the  $\nu_q$  spectrum (defined by (25) in the limit of infinitely small  $r$ ) does not coincide with the  $D_q$  spectrum of (14) and (15) (which do include the box counting and information dimensions as  $l^{(n)} \rightarrow 0$ ). Third, one cannot change probabilities and supports and expect scaling exponents to remain invariant: neither multifractal spectra  $f(\alpha)$ , nor generalized dimensions  $D_q$  derivable from multifractal spectra, can be used to define universality classes. The misconception that an optimal partition is unnecessary has led to the expectation that partitions can be manipulated without changing  $f(\alpha)$  and  $D_q$ . Multifractal spectra and generalized dimensions are nonuniversal: they change whenever either the support or the histograms on that support is changed. This is easily seen via the simplest possible examples.

To emphasize this last assertion we demonstrate what happens when we try to get a complete  $D_q$  spectrum by combining results from (12) and (13) for disjoint ranges of  $q$ , but while using

different distributions on different supports in each generating function. The underlying point set is in each case taken to be a finite number of points in the two-scale Cantor set. We consider first a uniform partition with uneven probabilities ( $p_1 > p_2$  in generation  $n = 1$ ) and statistical independence (for ease of calculation), whereas in the second case we take even probabilities  $p_1 = p_2 = 1/2$  also with statistical independence on the uneven but optimal partition with  $l_1 > l_2$ . We can cover the finite (or infinite) point set in the first case by using an efficient uniform (but not optimal) partition based on  $l_1$ , so that then we get  $D_\infty = \ln p_1 / \ln l_1$  and  $D_{-\infty} = \ln p_2 / \ln l_1$ . If in the second case, we use (13) with  $P_i = N_n^{-1} = 2^{-n}$ , then  $D_\infty = -\ln 2 / \ln l_1$  and  $D_{-\infty} = -\ln 2 / \ln l_2$ . The separate spectra do not lie on top of each other because the end points  $D_\infty$  and  $D_{-\infty}$  do not coincide. Clearly, we cannot combine these two different calculations in order to estimate disjoint parts of the  $D_q$  spectrum of either case.

## 5 Are galaxy distributions scale invariant?

In this search for scaling we use only the correlation “integrand”  $n_i(r)$ , not the correlation integral  $n(r)$  for the reasons explained in parts 3.6 and 4. We calculate the number of galaxies within a sphere of radius  $r$  centered on each galaxy as depicted in Figure 6. *We only use spheres that are completely within the sample geometry.* Since we want to investigate the scaling properties we are not allowed to apply any boundary corrections that assume stationarity of the distribution of galaxies with respect to translations (i.e. homogeneity) or rotations (i.e. isotropy). Such “corrections” would tend to introduce a spurious scaling with dimension three. Boundary “corrections” are inherent in all the usually used estimators for the two-point correlation function, see e.g. [60]. Similar corrections were used for estimators of the correlation integral see e.g. [49]. For the same reasons as above we use volume limited samples. Using flux (or magnitude) limited samples one is usually using a weighting scheme based on the selection function. In weighting with the selection function one assumes homogeneity in giving a weight to galaxies proportional to the mean density, which is determined mainly from the nearby regions.

We only show galaxies in the plots where we have at least one neighbour in a radius range larger than  $\Delta_r$ , our “scaling” range (with the limited data available it does not make sense to use decades, since we only have at maximum one decade available). To perform the scaling analysis more quantitatively we fit a straight line to the  $\log(n_i)$ - $\log(r)$  plot and determine the slope, again only for galaxies having a “scaling” range larger than  $\Delta_r$ .

We are severely limited by the small number density (or equivalently, the small sample size) of the catalogues. Therefore we will not be able to extend  $\Delta_r$  over more than one decade which is obviously too small to draw any conclusions about scaling (see Figure 1). To estimate the influence of  $\Delta_r$  on the distribution of the slopes we look at three different  $\Delta_r$ . To get a Geilo-range of scales from pie-shaped samples (as in figure 6) we would need observational data extending over several thousands  $h^{-1}\text{Mpc}$ .

### 5.1 The CfA I galaxy catalogue

We look, as an example of optically selected data, at the CfAI catalogue a magnitude limited catalogue consisting of 1880 galaxies (Huchra [33]). Using this data set fractal and multifractal analysis were performed e.g. by Coleman & Pietronero [13] or by Martinez et al. [48].

First consider the volume limited sample with  $40 h^{-1}\text{Mpc}$  depth with 360 Galaxies in total, having a mean separation of  $9.5 h^{-1}\text{Mpc}$ . In Figure 7 we show for 35 arbitrarily selected galaxies the number of neighbours  $n_i(r)$  against the radius of the sphere  $r$  for galaxies in the volume limited sample with  $40 h^{-1}\text{Mpc}$  depth. In this case we demand a “scaling” range of  $\Delta_r \geq 3.1 h^{-1}\text{Mpc}$ , resulting in 157 galaxies having a (more or less well) defined slope. In Figure 8 we show the scaling properties for 35 arbitrarily selected galaxies from the 67 galaxies with “scaling” range  $\Delta_r \geq 6.2 h^{-1}\text{Mpc}$ , and in Figure 9 we show the scaling properties of all the 22 galaxies which have a “scaling” range  $\Delta_r \geq 9.3 h^{-1}\text{Mpc}$ , spanning roughly one decade. As a first impression one recognizes that the scatter in the slope is large and does not decrease for larger  $\Delta_r$ , which should

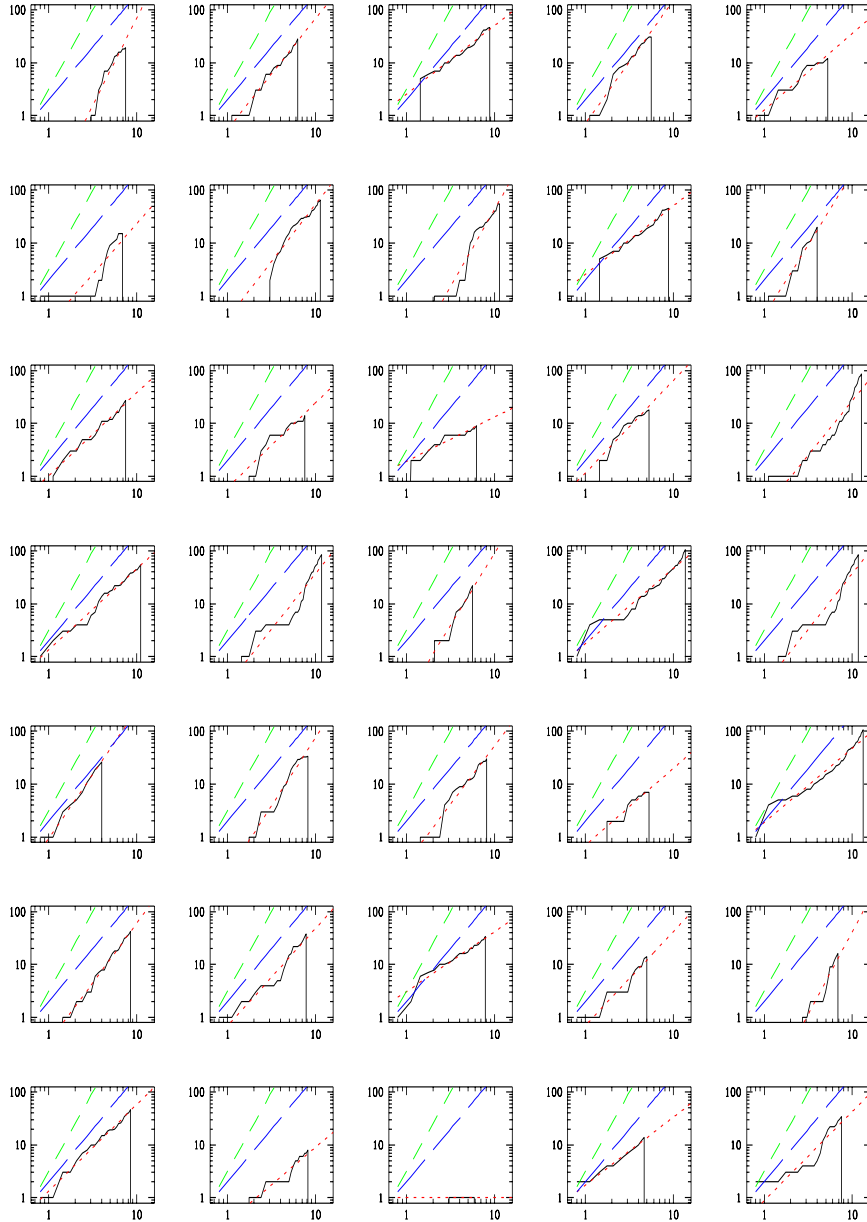


Figure 7: Plots of  $n_i(r)$  against  $r$  (logarithmic axes) for volume limited sample with  $40 h^{-1}\text{Mpc}$  depth (solid line) and "scaling" range  $\Delta_r \geq 3.1 h^{-1}\text{Mpc}$ . The dotted line is the fit, the long dashed line is for  $n_i(r) \propto r^2$  and the short dashed line for  $n_i(r) \propto r^3$ .

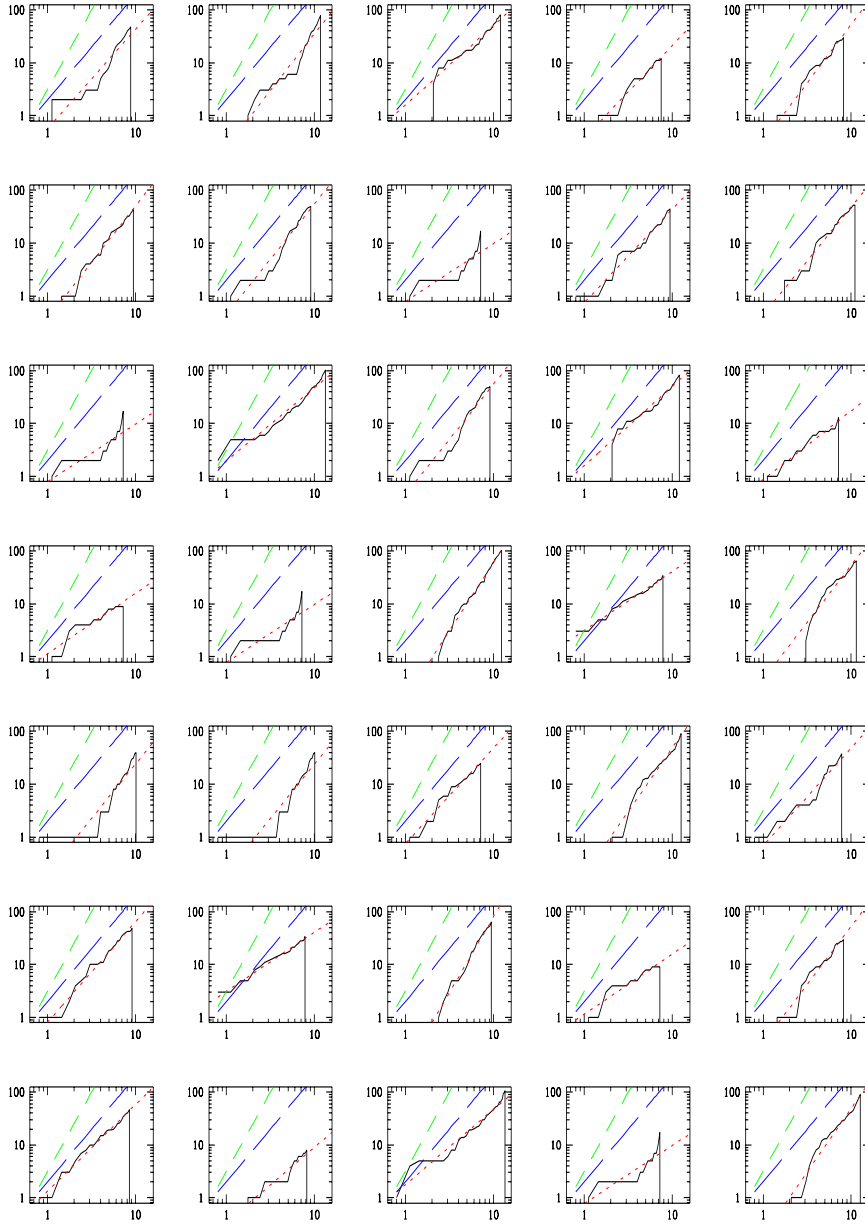


Figure 8: Same as Figure 7 but with "scaling" range  $\Delta_r \geq 6.2h^{-1}\text{Mpc}$ .

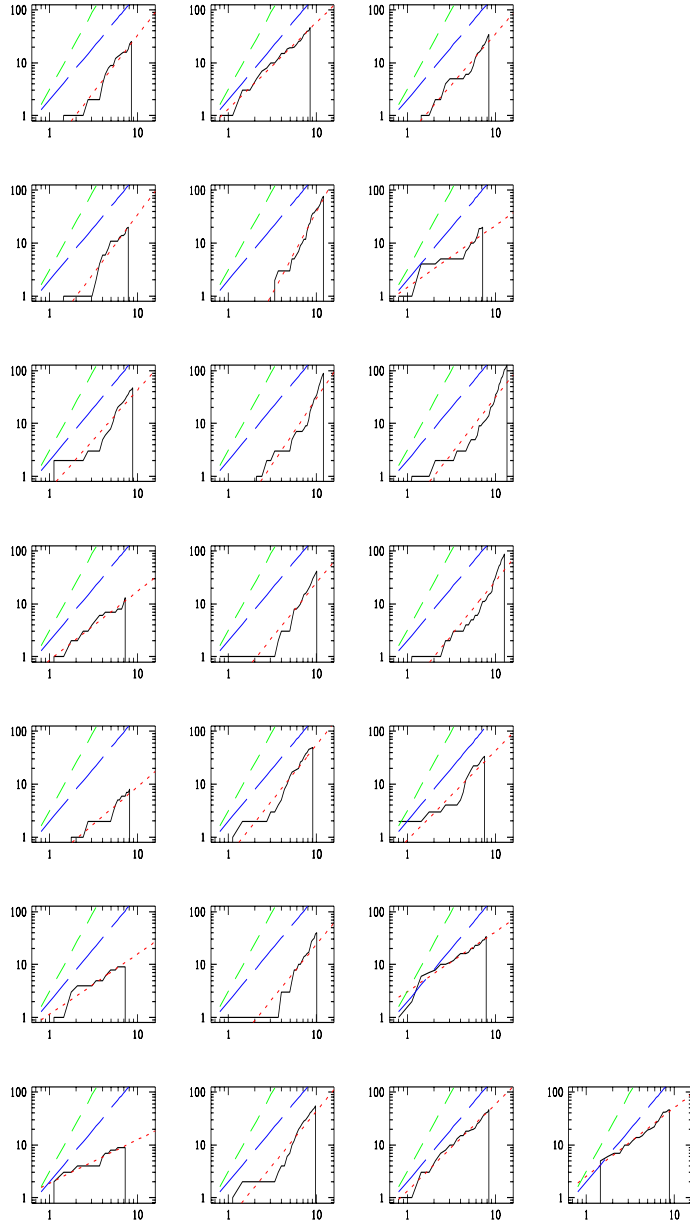


Figure 9: Same as Figure 7 but with "scaling" range  $\Delta_r \geq 9.3h^{-1}\text{Mpc}$ .

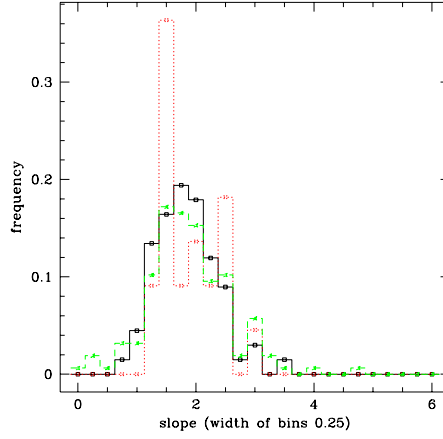


Figure 10: The frequency of the slopes for the volume limited sample with  $40 h^{-1}\text{Mpc}$  depth, for the sample with  $\Delta_r \geq 3.1 h^{-1}\text{Mpc}$  (stars), with  $\Delta_r \geq 6.2 h^{-1}\text{Mpc}$  (open squares), and with  $\Delta_r \geq 9.3 h^{-1}\text{Mpc}$  (crosses).

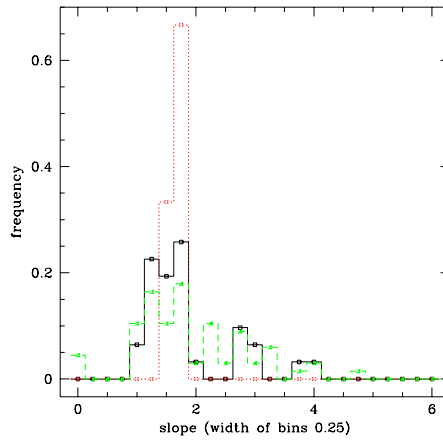


Figure 11: The frequency of the slopes for the volume limited sample with  $60 h^{-1}\text{Mpc}$  depth, for the sample with  $\Delta_r \geq 4.7 h^{-1}\text{Mpc}$  (stars), with  $\Delta_r \geq 9.4 h^{-1}\text{Mpc}$  (open squares), and with  $\Delta_r \geq 14.1 h^{-1}\text{Mpc}$  (crosses).

result in more reliable estimates for the slope. To make this impression more quantitative we plot the frequency of the slope for each of these samples in Figure 10. One has to bear in mind that this frequency table is in the case of  $\Delta_r \geq 9.3h^{-1}\text{Mpc}$  constructed from 22 galaxies only. In all three cases, the slope fluctuates over a range of 1.25 to 2.5.

In Figure 11 we plot the frequencies of the slopes for the volume limited sample with  $60 h^{-1}\text{Mpc}$ , consisting of 215 galaxies with mean separation  $24 h^{-1}\text{Mpc}$ . Imposing the constraints for the "scaling" range we are left with 67 galaxies for  $\Delta_r \geq 4.7h^{-1}\text{Mpc}$ , 31 galaxies for  $\Delta_r \geq 9.4h^{-1}\text{Mpc}$ , and only 9 galaxies for  $\Delta_r \geq 14.1h^{-1}\text{Mpc}$ . We see that no conclusions are possible with so few points. The peak around 1.75 for  $\Delta_r \geq 14.1h^{-1}\text{Mpc}$  (determined from only 9 galaxies!) is a mainly due to sampling galaxies from the same region of the space in the center of the sample (see Figure 6).

## 5.2 The IRAS 1.2 Jy galaxy catalogue

Now we look at a sample of IRAS selected galaxies with limiting flux 1.2 Jy Fisher et al. [23] consisting of 5313 galaxies. The big advantages of this sample is the nearly complete covering of the sky, and the homogeneous flux calibration. Fractal and multifractal analysis of IRAS galaxies were performed e.g. by Martinez & Coles [46], Xia et al. [80] and Labini et al. [72]. The last mentioned authors claim, that the IRAS samples are too sparse to estimate fractal dimensions reliably.

We proceed similar to the analysis of the CfA catalogue 5.1. As discussed in Kerscher et al. [41] we find differences between the northern and southern hemisphere, but since we do not want to focus on this topic we show the results for the combined data only.

In Figure 12 we show for 35 randomly selected galaxies the number of neighbours  $n_i(r)$  against the radius of the sphere  $r$  for galaxies in the volume limited sample with  $80 h^{-1}\text{Mpc}$  depth (mean separation of the galaxies is  $24 h^{-1}\text{Mpc}$ ). Restricting ourselves to a "scaling" range of  $\Delta_r \geq 6.3h^{-1}\text{Mpc}$  we are left with 359 galaxies of the total 788 galaxies in the volume limited sample. In Figure 13 we show the scaling properties for 35 randomly selected galaxies from the 167 galaxies with a "scaling" range of  $\Delta_r \geq 12.6h^{-1}\text{Mpc}$ , and in Figure 14 35 randomly selected galaxies from the 72 galaxies with a "scaling" range of  $\Delta_r \geq 18.9h^{-1}\text{Mpc}$ . Again we have a "scaling" range only spanning roughly one decade.

The sample with  $\Delta_r \geq 6.3h^{-1}\text{Mpc}$  is clearly inappropriate for an analysis, since often only one neighbouring galaxy is within the scaling range, giving rise to a spurious slope of zero. Again we see a large scatter in the slopes for all  $\Delta_r$ , which does not decrease if we go to higher  $\Delta_r$ .

To make this more quantitative we again plot histograms of the slopes, now for a sequence of volume limited samples. The sample with  $40 h^{-1}\text{Mpc}$  depth containing 646 galaxies is shown in Figure 15. The sample with  $60 h^{-1}\text{Mpc}$  depth containing 880 galaxies is shown in Figure 16. The sample with  $80 h^{-1}\text{Mpc}$  depth with 788 galaxies is shown in Figure 17.

## 5.3 Discussion of the results

In both catalogues the local scaling exponents  $\nu(i)$  fluctuate over a broad range (see Figures 15–17 and Figures 10, 11) indicating that there is *no* global monofractal scaling. It mainly tells us that the distribution admits large fluctuations. From the limited data we are not able to judge whether these fluctuations are scale invariant (over three decades) or not. Therefore, fractal scaling, and certainly multifractal scaling, cannot be deduced from that limited data as claimed in e.g. [13], [48], [46], [80], [72]. The fact that the correlation integral (or the two point correlation function) apparently scales with one exponent is in this case not related to the scaling of the galaxy distribution (again, see Figure 1). We want to emphasize that the broad range of different slopes is *not* a sign of multifractality, it only shows that we have large fluctuations. In e.g. [62] the authors claim to see scale invariance over three decades (from  $1 h^{-1}\text{Mpc}$  to  $1000 h^{-1}\text{Mpc}$ ). This statement is based on the scaling properties of only one  $n_i(r)$ . In this case  $n_i(r)$  should be the number of galaxies in a sphere centered on our galaxy. However, the analysis is carried

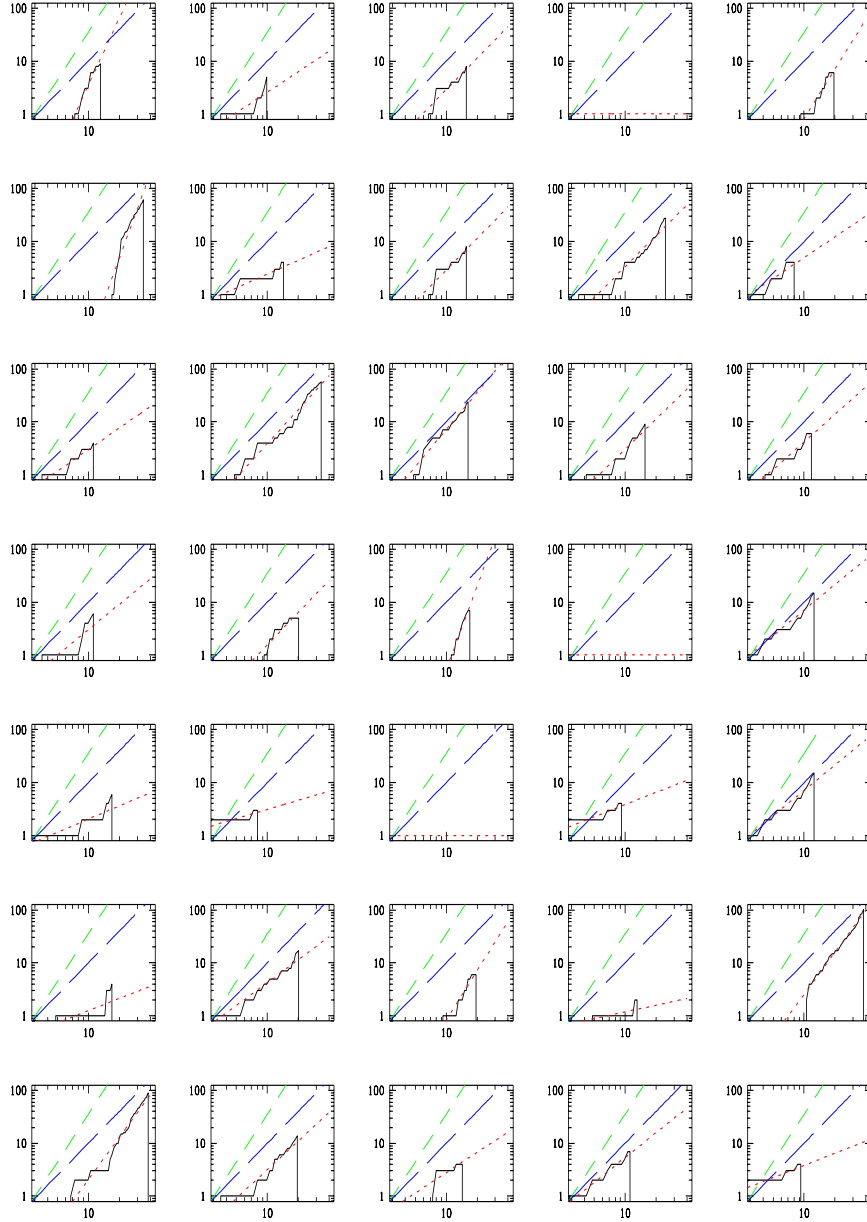


Figure 12: Plots of  $n_i(r)$  against  $r$  (logarithmic axes) for volume limited sample with  $80 h^{-1}\text{Mpc}$  depth (solid line) and "scaling" range  $\Delta_r \geq 6.3h^{-1}\text{Mpc}$ . The dotted line is the fit, the long dashed line is for  $n_i(r) \propto r^2$  and the short dashed line for  $n_i(r) \propto r^3$ .



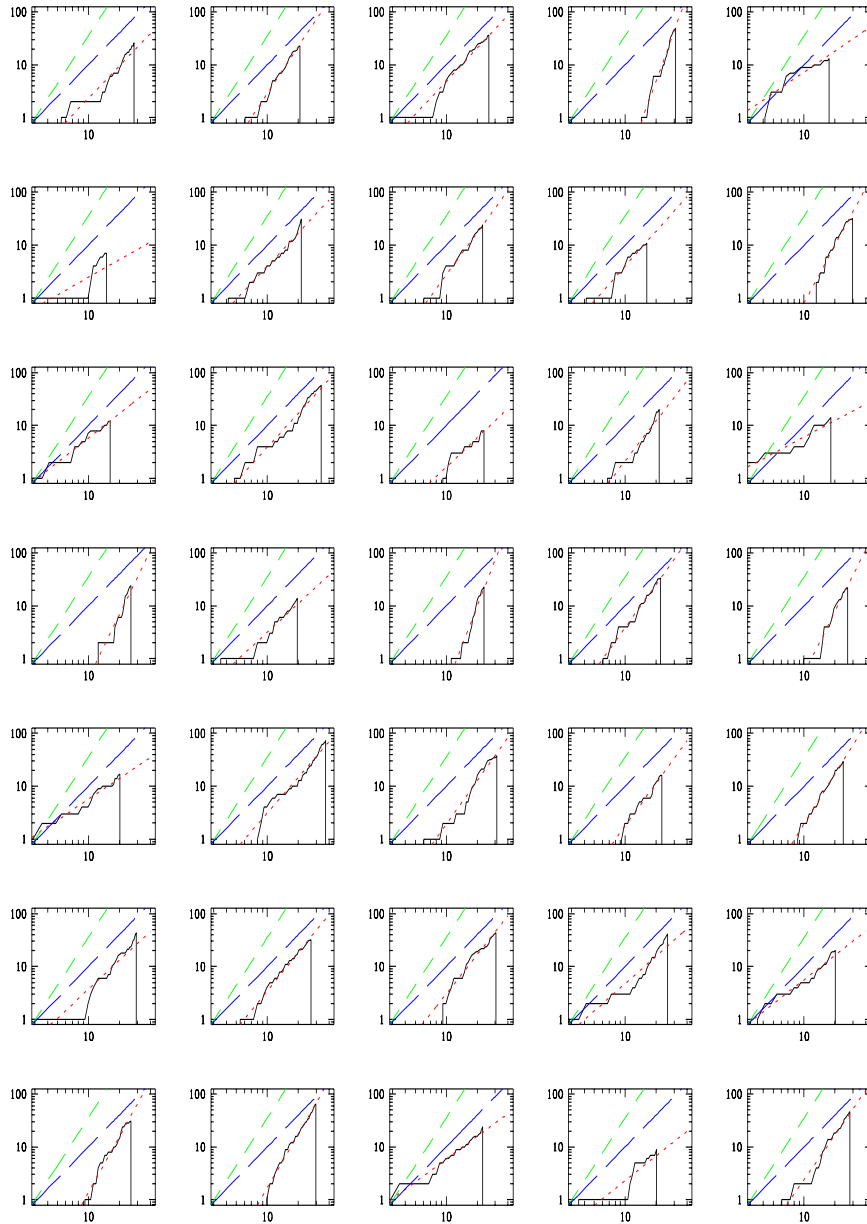


Figure 13: Same as Figure 12 but with "scaling" range  $\Delta_r \geq 12.6h^{-1}\text{Mpc}$ .

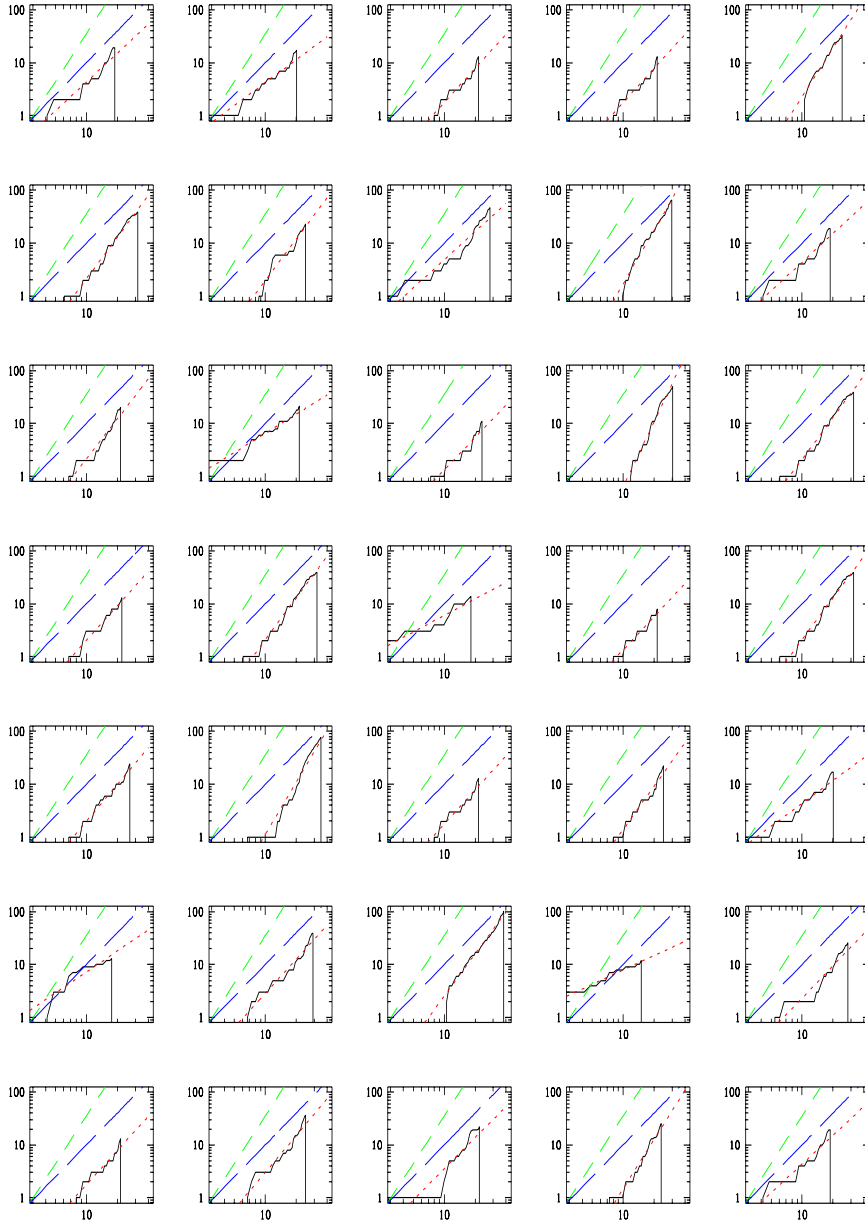


Figure 14: Same as Figure 12 but with "scaling" range  $\Delta_r \geq 18.9h^{-1}\text{Mpc}$ .

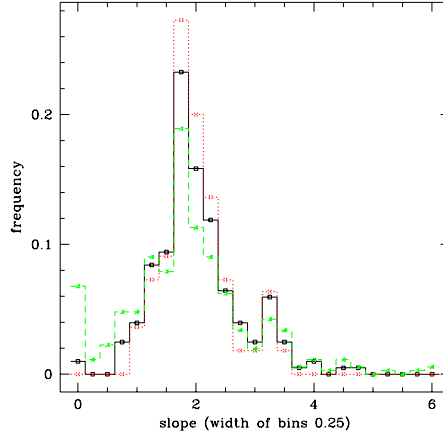


Figure 15: The frequency of the slopes for the volume limited IRAS sample with  $40 h^{-1}\text{Mpc}$  depth, for the sample with  $\Delta_r \geq 3.1 h^{-1}\text{Mpc}$  (stars), with  $\Delta_r \geq 6.2 h^{-1}\text{Mpc}$  (open squares), and with  $\Delta_r \geq 9.3 h^{-1}\text{Mpc}$  (crosses).

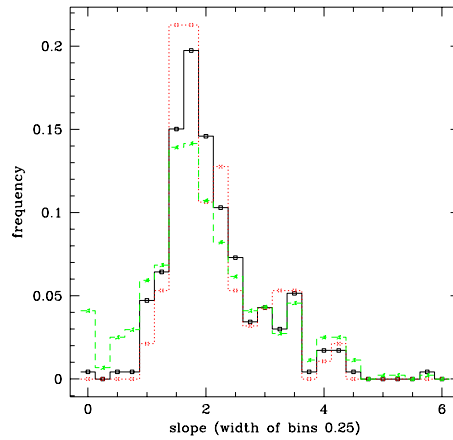


Figure 16: The frequency of the slopes for the volume limited IRAS sample with  $60 h^{-1}\text{Mpc}$  depth, for the sample with  $\Delta_r \geq 4.7 h^{-1}\text{Mpc}$  (stars), with  $\Delta_r \geq 9.4 h^{-1}\text{Mpc}$  (open squares), and with  $\Delta_r \geq 14.1 h^{-1}\text{Mpc}$  (crosses).

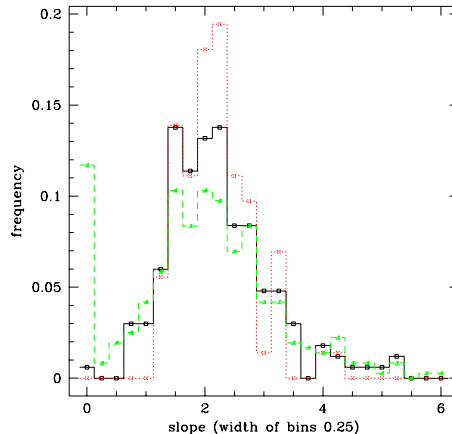


Figure 17: The frequency of the slopes for the volume limited IRAS sample with  $80 h^{-1}\text{Mpc}$  depth, for the sample with  $\Delta_r \geq 6.3h^{-1}\text{Mpc}$  (stars), with  $\Delta_r \geq 12.6h^{-1}\text{Mpc}$  (open squares), and with  $\Delta_r \geq 18.9h^{-1}\text{Mpc}$  (crosses).

out by using only intersections of a cone with a sphere as discussed in [72]. Such an analysis is inconsistent with their own definition of fair sampling, very badly violating Fig. 8 of [13].

In fitting straight lines to a log-log plot over roughly one decade we have performed a superficial data analysis, one that gives excessive weight to galaxies near the center of the sample. Unfortunately nothing more is possible without postulating “boundary corrections” that have no basis in observation, or without even more unfairly weighting points near the center of a conical sample more heavily than those near a boundary. But even in doing so, we do not find any indication of global scaling. The main message is that the current data are insufficient for a reliable scaling analysis. We end this section with a quote from [13]: “...if a sample contains too few points there may be no way to get any information from it. In such a case one has to wait for better (observational) data.”

## 6 Generating functions

The term multifractal is defined in Jones [36] by requiring only that the moments of an arbitrary distribution  $P(X, l)$ ,

$$\langle X^{q-1} \rangle = \sum_X P(X, l) X^{q-1}, \quad (31)$$

where  $X$  is a random variable defined in or on intervals of size  $l$ , should scale,

$$\langle X^{q-1} \rangle \approx l^{\zeta_q}, \quad (32)$$

for small enough interval sizes  $l$ . However, without further requirements on  $X$  and  $P(X, l)$ , there is no reason to expect that scaling exponents in (32), if they exist *at all* for a given distribution  $P(X, l)$ , bear any relation to generalized dimensions  $D_q$  derivable in the infinite precision limit from multifractal spectra  $D(\lambda)$  or  $f(\alpha)$ . To be specific, is the partition nonoverlapping? Efficient? What is fractal about  $X$  or  $P(X, l)$ ? We will show via example in part 7 that equation (31) with a scaling law (32) generally does not describe intermittence due to voids, and that if one tries in those cases to force the definition  $\zeta_p = (p-1)D_p$  (or, as in [36],  $\zeta_p = (1-p)D_p$ ) then the  $D_p$  are not dimensions describing the support of the probability distribution, or of any other coarsegrained set or subset connected with an arbitrary distribution  $P(X, l)$ .

The generating function (31) combined with the scaling expectation (32) is used in definitions of *multiaffine* fractals ([5]), where a deterministic or random variable (or field)  $X$  is continuous but has singular (or no) derivatives. If the distribution of singularities of the field  $X$  can be described locally by writing  $X \approx l^h$  and  $P(X, l) \approx l^{-f(h)}$ , then (31) may or may not yield scaling exponents  $\zeta_p$  that give rise to a spectrum of generalized dimensions, defined by  $(p-1)D_p = ph(p) - f(h(p))$  in the limit  $l \rightarrow 0$ , where  $D_0, D_1$  and  $D_2$  really are *fractal dimensions of something* in the model. This happens *only* when  $f(h)$  describes a spectrum of fractal dimensions. Otherwise  $h$  and  $f(h)$  are just a rewriting of a nonfractal probability distribution  $P(X, l)$  via a coordinate transformation, and *nonfractal distributions cannot be made fractal (or the converse) by a differentiable coordinate transformation*. Stated another way,  $f(h)$  is not a spectrum of Hausdorff dimensions unless “ $l$ ” represents an optimal or at least efficient partition of the support of an underlying pointwise distribution  $P(x)$ . Examples in the literature where  $X \approx l^h$  with  $P(X, l) \approx l^{-f(h)}$  are used without any requirement of efficient partitioning of a support are height fluctuations in surface roughening ([5]), self-organized criticality ([40]) and velocity structure functions in the inertial range of fluid turbulence ([24]). In contrast with multiaffine fractals (where there is no idea of a generating partition), for a self-similar fractal (heretofore called “fractal”) the point set is generally spatially-fragmented (Koch and Peano curves are, however, continuous), like a Cantor set, and  $P_i$  scales like  $l_i^{\alpha_i}$  (not like  $l_i^{-f(\alpha_i)}$ ) in order to describe a highly singular density  $\rho_i = P_i/l_i = l_i^{\alpha_i-1}$  on the optimal partition describing the support of  $P(x)$ .

In a spirit similar to the attempt to define multifractal by using the moments (31) of an arbitrary distribution  $p(X, l)$  with a scaling law (32), the definition

$$\langle P^{q-1} \rangle = \sum_P p(P, l) P^{q-1}, \quad (33)$$

where the probability distribution  $p(P, l)$  is undefined, is treated in various places ([14]) as if it would be identical with the generating function

$$\chi_n(q) = \langle P^{q-1} \rangle_{\text{coarsegrained}} = \sum_{i=1}^{N_n} P_i P_i^{q-1}, \quad (34)$$

although it is not.

For an arbitrary probability distribution  $p(P, l)$  these two generating functions are not even related; their scaling exponents (if scaling exponents exist in either case) are not necessarily the same even if the generating functions *are* qualitatively related. *Multifractal spectra and generalized dimensions are not universal*. Instead, they change with the histograms and their support. Furthermore, any deviation from the empirical distribution  $P(x)$  and its optimal coarsegrained descriptions  $\{P_i\}$  is equivalent to changing the underlying data set. Rather than imagining that the empirical distribution  $P(x)$  can be treated as a random field that fluctuates from one galaxy sample to the other (as in Jones [35]), we view different  $P(x)$ 's from different samples as disjoint pieces of a *single* global distribution of galaxies whose local properties can be discovered empirically, but whose entire global (one hesitates to say “universal”) aspect can never be known due to the inherent limitations on observation. We do not want to try to replace what we do not know ( $P(x)$  *measured* globally) with speculations that cannot be tested ( $p(P, l)$  *postulated* globally). The notion of statistical ensembles is useless here: There is only one universe, and it is not in equilibrium.

The source of confusing together entirely different generating functions can be traced to the use of the infinite precision limit in papers on dynamical systems theory written more than ten years ago. It is suggested in [31] (see also [27]) that (34) is analogous to the Lebesgue integral

$$\langle P(B_l(x))^{q-1} \rangle = \int dP(x) P(B_l(x))^{q-1} \quad (35)$$

and should yield the same generalized dimensions  $D_q$  in the infinite precision limit, where  $P(x)$  is supposed to be “the natural invariant measure” of a chaotic dynamical system on a strange

attractor (see [29], e.g., for one definition of “natural”) and  $P(B_l(x))$  is the fraction of points lying within a ball of size  $l$  covering (but not necessarily centered on) a data point  $x$ . There are two serious difficulties with the attempt to replace (34) by (35), and both revolve about lack of uniqueness.

First, there is no evidence from observation that a chaotic dynamical system generates “a natural measure” for the various initial conditions (meaning also “present conditions”) found in nature. Mathematically seen, a chaotic dynamical system can generate infinitely many different distributions (“measures”)  $P(x)$  for infinitely many different classes of initial conditions ([53] & [54]). Empirically, the dependence on initial conditions is not a problem: the data are described by the empirical staircase

$$P(x) = \frac{1}{N} \sum_{i=1}^N \Theta(x - x_i). \quad (36)$$

Without having made any theoretical assumptions that prejudice the data analysis we can say that the initial conditions, whatever they were, produced the empirical distribution  $P(x)$  via the time evolution of some dynamical system.

Given the empirical measure (36) there is still ambiguity inherent in the attempt to use (35) as a replacement for (34). In finite precision there are different possible definitions of the integral, depending on which subset of the data set we decide to measure (before we can identify the function  $P(B_l(x))$  we must first define “ $l$ ”).

If we choose the balls/intervals  $B_l(x)$  to have arbitrary length  $l$ , centered on a data point  $x_i$  (as in [59]), then the fraction of points lying within each interval of size  $l$  is given by  $P(B_l(x)) = n(x, l)$  where  $n(x_i, l) = n_i(l)$  is the correlation integrand

$$n_i(r) = \frac{1}{N} \sum_{i,j=1;i \neq j}^N \theta(l - |x_i - x_j|). \quad (37)$$

Deleting the term  $j = i$  in (37) is unimportant if the intervals are large enough to give “good statistics” (pedantically, one can also replace the factor  $1/N$  by  $1/(N - 1)$  in (37)). Insertion of the pointwise definitions  $P(B_l(x)) = n(x, l)$  and

$$dP(x) = \frac{dx}{N} \sum_{i=1}^N \delta(x - x_i) \quad (38)$$

into the integral (35) yields the correlation integral generating function

$$\int dP(x) P(B_l(x))^{q-1} = \frac{1}{N} \sum_{i=1}^N n_i(l)^{q-1} = G_n(q), \quad (39)$$

which differs significantly from (34) in data analysis, as we have emphasized in section 4.

In dynamical systems theory the  $N$  intervals can in principle be chosen small enough not overlap with each other: on a mathematically-defined strange attractor there are  $t^\infty$  points in any neighborhood of any arbitrary point  $x_i$  on the attractor ( $t^\infty$  is the cardinality of the attractor). Here, the  $N$  intervals (or balls)  $B_l$  of size  $l$  can be chosen small enough not to overlap, but certainly do not partition the attractor efficiently, if at all. Equation (39), which was not invented with partitioning in mind, is merely a time average over  $N$  points on the attractor, and the uniform weight  $1/N$  is correct because each point  $x_i$  occurs exactly once (so long as trajectories of the dynamical system are unique, which we assume here). In nonlinear dynamics calculations the number  $N$  of points may be increased by increasing the precision of the calculation. In cosmology, in contrast,  $N$  is the total number of galaxies in a finite sample, so that the  $N$  intervals of size  $l$  are always overlapping.

There is a different way to define balls  $B_l(x)$  and a corresponding function  $P(B_l(x))$ . Instead of choosing  $N$  uniform intervals where  $N$  is the number of data points, requiring the pointwise

definition  $P(B_l(x)) = n(x, l)$  as given by (37) (which does *not* include a partition of the data set), we can instead choose our balls  $B_l$  to be the  $N_n$  intervals  $\{l_i\}$  in the optimal partition of the data. Then,  $P(B_l(x))$  is given by the simple function

$$P(B_l(x)) = \sum_{i=1}^{N_n} P_i \chi_{l_i}(x) \quad (40)$$

where  $\chi_{l_i}(x)$  is the characteristic function for the partition  $\{l_i\}$  of disjoint intervals [66] and

$$P_i = P(x_i + l_i) - P(x_i) = \sum_{j=1}^{i+n_i-1} \theta(x_{i+n_i} - x_j) = n_i/N \quad (41)$$

Here,  $x_i$  and  $x_{i+n_i} = x_i + l_i$  are taken to be the end points of any of the  $N_n$  *optimal* intervals  $\{l_i\}$ . With this optimal choice of “what to measure” (optimal choice of function  $P(B_l(x))$  to integrate with respect to the measure  $P(x)$ ) the integral (35) yields

$$\int dP(x) P(B_l(x))^{q-1} = \sum_{i=1}^N P_i P_i^{q-1} = \chi_n(q), \quad (42)$$

*From the standpoint of both data analysis and measure theory the only significant difference between the distributions (37) and (41) is the lack of a partition in (37), and the use of an optimal partition to define (41). Whether these two approaches do or do not, in the limit of  $l^{(n)} \rightarrow 0$  for a mathematical fractal of cardinality  $t^\infty$ , yield the same generalized dimensions (whether  $D_q = \nu_q$  as  $l^{(n)} \rightarrow 0$ ) is of no importance whatsoever for the analysis of empirical data.*

## 7 Lognormal distribution

What has lognormal to do with multifractal? The question arises because it has been asserted that the lognormal distribution is multifractal, that it defines a spectrum of generalized dimensions ([37] & [36], [35]) and an  $f(\alpha)$  spectrum ([24]). Before answering this question we review how and where the lognormal distribution appears in discussions of multifractals, where a multifractal spectrum (as defined in this paper, following Halsey [30]) describes the spectrum of dimensions of nonoverlapping subsets of the support of a probability distribution.

With the discussion of [37] in mind, but following [30], let us make a largest term approximation on the generating function (12). With  $q$  fixed we first locate the largest term in (12) by minimizing the exponent  $(q\alpha - f(\alpha))$ , yielding  $q = f'(\alpha(q))$ . Very near (and only very near) to the smallest exponent  $\tau(q) = (q\alpha(q) - f(\alpha(q)))$ , where  $\alpha(q) = \tau'(q)$ , we can write  $f(\alpha) \approx \tau(q) + (\alpha - \alpha(q))^2 f''(\alpha(q))/2$ . According to a standard method ([7]) we next replace the sum over all these nearby terms by the integral

$$\chi_{n(q)} \approx l^{(n)\tau(q)} \int_{\delta\alpha} d\alpha \rho(\alpha) \left( l^{(n)} \right)^{(\alpha - \alpha(q))^2 f''(\alpha(q))} \quad (43)$$

where the range of integration  $\delta\alpha$  is over the tiny region  $\delta\alpha$  in  $\alpha$  containing all of the exponents  $(q\alpha - f(\alpha))$  that do not deviate from the minimum exponent  $\tau(q)$  more than quadratically in  $(\alpha - \alpha(q))$ . This quadratic approximation to deviations of the exponent  $(q\alpha - f(\alpha))$  from the minimum  $\tau(q)$  only works as  $l^{(n)} \rightarrow 0$ , in which case the integrand in (43) is sharply enough peaked that, with small error, we may extend the integration limits to plus and minus infinity. Clearly, a locally (not globally) Gaussian approximation to deviations from the minimum exponent  $\tau(q)$  is the same as saying that the deviations of  $(N(\alpha) (l^{(n)})^q \alpha)$  from  $(l^{(n)})^\tau(q)$  are locally (not globally) lognormal. This local lognormality only contributes to the *prefactor* in (43) in the unphysical limit where  $l^{(n)} \rightarrow 0$ , and not to the  $f(\alpha)$  spectrum described by the exponent  $\tau(q)$ . Any time that an exponent  $h$  has a Gaussian distribution then the function  $p(h) = l^h$  is distributed lognormally (see

[52] for an example from percolation theory, where permeabilities  $\kappa$  of sandstone and limestone deposits were long thought to be approximately lognormally distributed, with Gaussian porosities  $\phi$ , where  $\kappa \approx l^\phi$ . *This has nothing to do with the question whether the lognormal distribution is multifractal.*

There are two ways, *related mathematically to the above approximation*, in which the lognormal distribution is called multifractal in [36] and [37]. Jones [36] asserts that (31) with (32) defines multifractal, where  $\zeta_p = -(p-1)D_p$  and the  $D_p$  are supposed to be generalized dimensions derivable from the Halsey method as well. *This constitutes an entanglement of unrelated ideas.* Following Jones [36], we use  $X = l^h$  in (31) along with a lognormal distribution of  $X$  to compute  $\langle l^{ph} \rangle$  (the exponent  $h$  is Gaussian with mean  $\langle h \rangle$  and mean square fluctuation  $\sigma^2 = \langle (h - \langle h \rangle)^2 \rangle$ ). Using Jones's [36] second definition of  $\zeta_p$  (instead of his first), where  $\zeta_p = \ln(\langle X^p \rangle) / \langle X \rangle^p$ , we obtain  $\zeta_p = \exp(2\sigma^2 \ln l) p(p-1)$ . In other words a scaling law (32) generally does *not* follow: lognormal distributions per se, inserted into (31) do not yield scale invariance (32), because the expected scaling exponent depends on  $\ln l$ . A scaling law (32) follows *only* if we restrict to lognormal distributions where  $\sigma^2$  is proportional to  $-1/\ln l$ . In this case we obtain  $D_p = -\langle h \rangle p$ , where  $D_2 < D_1 < D_0 = 0$ .  $D_0 = 0$  is not the dimension of the support of the lognormal distribution (where  $D_H = 1$ ), and the scaling exponents  $D_p$  are not the dimensions of anything else in that distribution. (We adhere to the assumption that fractals and multifractals are generated by deterministic dynamics, and do not consider the so-called "random fractals".) Jones's refinement of (32) is, in this case, equivalent to the imposition of the constraint  $\zeta_1 = 0$  in turbulence modelling (see Frisch [24]).

To try to model an eddy cascade in fluid turbulence one must evaluate the average  $\langle l^{ph} \rangle$  where  $l$  represents the size of an  $n$ th generation eddy, and  $h$  is supposed to be an exponent analogous to  $\alpha$  in multifractal spectra. There, Frisch [24] makes a different identification than Jones, namely, that  $(p-1)D_p = \zeta_p + 3(p-1)$  for a lognormal distribution. This yields  $D_0 = 3$  (space-filling support) but the exponents  $D_p$  for  $p \neq 0$  are not dimensions of anything in the model. The origin of this apparent (from our standpoint) mislabeling of scaling exponents as multifractal is that Frisch defines  $f(\alpha)$  spectra (and consequently  $D_p$  spectra) differently than we have. His definition is not designed to agree with the fractal dimensions  $f(\alpha)$  describing singular distributions ala Halsey et al. [30], but describes instead the *Cramer function* in statistics ([43]). *A Cramer function may exist where nothing is fractal.* A Cramer function, by construction, describes distributions of independent random variables  $h_i$  or  $\alpha_i$  the limit where  $n$  goes to infinity ( $l$  goes to zero). In contrast, the indices  $\alpha$  in (12) and (41) are not random variables: they are scaling indices describing coarsegrained probabilities (and occupation numbers  $n_i = NP_i$ )  $P_i = l_i^{\alpha_i}$ .

The Cramer function is a systematic way of obtaining a description whereby  $X \approx l^h$  and  $P(X, l) \approx l^{-f(h)}$  via a limit theorem in classical statistics, *for the case where the  $h_i$  are independent random variables*, and has no necessary connection with the idea of spectra of Hausdorff dimensions, or generalized dimensions derivable from spectra of Hausdorff dimensions. The Cramer function is based on the law of large numbers and appears in classical equilibrium statistical mechanics, for example. This approach can be used to describe an alternative version of lognormality discussed in [37]: in that case their spectrum  $f(a) \approx D_0 - (\alpha - \alpha_0)^2 / 4(\alpha_0 - D_0)$  describes the *integrand* of (31), and not a scaling law (32) that might follow as a consequence of actually *calculating* the integral (31). A scaling law (32) does not follow at all without assuming arbitrarily that  $\sigma^2$  varies as  $-1/\ln l$ . With that restriction we obtain  $(p-1)D_p = \zeta_p - (p-1)D_0$  with  $\zeta_p = -\alpha_0 p$ , analogous to Frisch's result quoted above, but where we should now choose  $D_0 = 1$  in order to describe the support of the lognormal distribution (otherwise,  $D_0$  is not the fractal dimension of anything in the model). Even with this choice the remaining  $D_p$  are not fractal dimensions, even for  $p = 1, 2$ , of any aspect of the lognormal distribution. However, the *same* lognormal distribution can be understood from an entirely *different* standpoint: namely, as a combination of the Gaussian integrand with the exponent  $\tau(0) = -D_0$  in equation (43) of Halsey et al above. In this case  $D_0$  is *not* the Hausdorff dimension of the support of the lognormal distribution, and the linear spectrum  $D_p$  describes *only* the region near the peak of an unknown  $f(\alpha)$  spectrum, a spectrum of box-counting dimensions where  $f_{\max} = D_0$  (from the standpoint of eqn. (43) above one would interpret the  $\zeta_p$  spectrum derived from the lognormal distribution in



turbulence modelling as the fragment of an  $f(\alpha)$  spectrum that is valid only for very small values of  $p$ , near  $p = 0$ , although this is certainly *not* the traditional interpretation). On the other hand, however, the *generalization* of the lognormal approximation represented by Jone’s [35] equations (14) and (15), and (30), are not definitions of  $f(\alpha)$  ala Halsey et al. [30], but represent instead the idea of a Cramer function in classical statistics (see Frisch ’95): *unless  $f(\alpha)$  arises as the spectrum of Hausdorff dimensions from an infimum condition on partitions, then  $f(\alpha)$  is not (by the Halsey [30] definition) a multifractal spectrum*. This entanglement of different ideas did not originate in cosmology: one of the authors of Halsey et al. [30] later used the Cramer function, called it “multifractal”, and cited Halsey et al. [30] as the reference ([40]).

One can choose to follow Halsey et al. [30] in defining  $f(\alpha)$  and  $D_q$ , or one can follow Mandelbrot [43] in defining “ $f(\alpha)$  and  $D_q$ ” via Cramer functions [24], but one should not mix these two different definitions together without comment as is done in [36]. We recommend the definition of multifractal given in this paper as the standard because, in that case,  $f(\alpha)$  is always the Hausdorff dimension of a subset of the support of the empirical distribution  $P(x)$ . The necessity of an optimal partition in order to define  $f(\alpha)$  is implicit in Halsey et al. [30] (see their “infimum” requirement) but was not emphasized strongly enough at that time. The role played by the infimum requirement became clear only after the later work on generating partitions in nonlinear dynamics ([21], [16] and [64]), which is little-known within the community of cosmologists.

When is a distribution  $P(x)$  multifractal? To answer this question consider any distribution  $P(x)$ , empirical or theoretical, where  $P(0) = 1/N$ ,  $P(1) = 1$ , and  $P(x)$  is nondecreasing. For idealized differentiable distributions we have  $N = 2^\infty$  (which is the same as  $10^\infty$ , etc.) and  $P(0) = 0$ .  $P(x)$  need not be differentiable, however, and generally isn’t. In order to determine whether  $P(x)$  “is multifractal” (admits a decomposition of its support into interwoven fractals with different dimensions  $f(\alpha)$ ) one must determine the optimal partition and form the difference  $\Delta P(x)$  over each interval in that support to obtain the hierarchy of histograms  $\{P_i\}$  (for a differentiable distribution any space-filling partition will do the job). Having done that, one then investigates whether  $P_i \approx l_i^{\alpha_i}$  holds over  $N(\alpha) \approx l^{-f(\alpha)}$  intervals in the support as the interval sizes are systematically reduced. All fractal distributions (for points on a line) have an density  $\rho_i \approx l_i^{\alpha_i - 1}$  that is dense with singularities because  $\alpha_i < 1$ , and if the distribution is multifractal then the indices  $\alpha_i$  will vary over the support according to  $N(\alpha) \approx l^{-f(\alpha)}$ . A highly fragmented (spiky) coarsegrained density is typical of a multifractal distribution  $P(x)$ .

Gaussian distributions are not multifractal. Neither are lognormal distributions. No smooth, differentiable distribution is multifractal because, by definition, such a distribution has a smooth density on a support with integer dimension  $D_0$ . Smooth distributions can be differentiated everywhere, corresponding to the requirement that  $f(\alpha) = \alpha = D_0$  holds everywhere. The Cantor function  $P(x)$  in part 3.5 describes clustering and voids), the binomial distribution with  $p_1 \neq p_2$  on a space-filling support describes intermittence without voids (see [56] for a physical example), but the lognormal distribution cannot describe voids because it is differentiable. The distribution defined by the density  $\rho(x) = dP(x)/dx = (x(1-x))^{-1/2}$  is not differentiable at  $x = 0$  and 1 and is bifractal (Halsey et al. [30]):  $\alpha = f(\alpha) = 1$  for  $0 < x < 1$  but  $\alpha = 1/2$ ,  $f(\alpha) = 0$  for  $x = 0$  and 1. The bifractal staircase of She et al. [69] shows coalescence without voids only because a continuum of initial conditions was used rather than a finite number (blocks of initial conditions with voids should also produce coalescence with voids in that model).

Summarizing, nontrivial  $f(\alpha)$  spectra guarantee an intermittent probability density, one corresponding to a nondifferentiable probability distribution  $P(x)$ . All fractal distributions have singular densities. Having a fractal support guarantees a singular density  $\rho \approx l^{\alpha - 1}$  with  $0 < \alpha < 1$ , but multifractal scaling can also hold for inhomogeneous distributions (like those having statistical independence with uneven probabilities) on a space-filling support.

## 8 Homogeneity, coarsegraining and hydrodynamics

The singular “pointwise” density of matter  $\rho(x, y, z)$  in any epoch is determined by the empirical staircase distribution  $P(x, y, z)$ , the generalization of (7) to three dimensions. A necessary but

*insufficient* condition for a coarsegrained density that is smooth enough to be approximable by a differentiable function is that the support of the empirical distribution is space-filling, meaning  $D_H = 3$ .

No information about  $D_H$  is provided by the correlation integral exponent  $\nu$  (or by the correlation dimension  $D_2$ ) unless, (1) the support is monofractal and the distribution is uniform ( $\alpha = f(\alpha) = D_H < 3$ ), or (2) the support is space-filling and the distribution is uniform or at least differentiable ( $\alpha = f(\alpha) = D_H = 3$ ). In both cases  $\nu = D_2 = D_H$ . Otherwise, we know only that  $\nu < D_H$  and  $D_2 < D_H$ . An increase in  $\nu$  with an increase in scale from intermediate toward cosmologic scales,  $l^{(n)} \gg 1000h^{-1}\text{Mpc}$ , even if it would be found in the data, would not tell us anything about  $D_H$  unless we would find that  $\nu = 3$ . So long as  $\nu < 3$  no information about  $D_H$  is provided by  $\nu$ . An increase of  $\nu$  with increasing scale (as is claimed in [50], [8]) would not imply that there exists a large scale coarsegraining where  $D_H = 3$ . If  $D_H < 3$  then the approximation of the empirical distribution by a differentiable one is impossible. The same conclusion follows if  $\nu < D_H = 3$ .

Fractal scaling of galaxies in an intermediate range  $1 \leq r \leq 1000h^{-1}\text{Mpc}$ , e.g. would still allow for the possibility of nonfractal matter distributions at the largest (or “cosmologic”) scales. An empirical matter distribution  $P(x, y, z)$  that shows no clusters and voids “at large enough scales”  $l^{(n)}$  would require a support with dimension  $D_H = 3$ . Whether galaxies are distributed more or less uniformly over a nonuniform space-filling support  $\{l_{x,i}l_{y,i}l_{z,i}\}$  is then a question of whether  $P_i \approx l_{x,i}l_{y,i}l_{z,i}$  holds over enough generations of the hypothetical “cosmologic-scale support” so that one can define the derivatives of densities normally used in hydrodynamics. Only for a uniform support would this condition reduce to the requirement of statistical independence with equal probabilities,  $P_i \approx N_n^{-1}$ . This is the requirement for large-scale uniformity ( $\rho(x, y, z) \approx \text{constant}$ ) stated in the language of dynamical systems theory.

A necessary condition for homogeneity in a given direction  $x$ , at cosmological scales  $l^{(n)} \gg 1000h^{-1}\text{Mpc}$ , can also be stated as follows: on what scale  $l^{(n)}$  of cosmologic coarsegraining can a staircase  $P(x)$  of  $N$  steps ( $P(x)$  denotes the empirical distribution  $P(x, y, z)$  with  $y$  and  $z$  held constant) be approximated by a differentiable distribution,  $P'(x) \approx \rho(x)$ , where  $\rho(x)$  is smooth, approximately analytic? There are two requirements: the number  $n_i$  of data points in each interval must be very large, and the spacing between points cannot be very different from  $\Delta x \approx 1/N$ . This is the same as saying that the steps in  $P(x)$  are nearly uniform and of very small width, and lie approximately on the straight line  $P(x) \approx x$  with slope  $\rho(x) \approx 1$  (uniform density). If the pointwise spacing is not exactly  $\Delta x \approx 1/N$ , but  $D_H = 3$  and there are no voids and clustering, then the staircase may be a smooth deformation of the constant density distribution  $P(x) \approx x$  with variable but nearly smooth slope  $\rho(x) \approx P'(x)$  approximating a nonuniform smooth density. The necessary and sufficient condition for large-scale homogeneity, stated in the language of statisticians is given in Stoyan et al. [70]. Contrary to the advice of part 9 in [13] we point out that “pencil beam surveys” generally cannot be treated as one-dimensional cuts. In order to qualify as a one dimensional cut, the maximum width of a pencil beam survey should be on the order of the size of a galaxy.

If we think in terms of hydrodynamic models of clustering, then space-filling supports, by Liouville’s theorem, require conservative dynamical systems. A smooth density at large scales cannot be the result of dissipative hydrodynamics.

No empirical test can be performed globally on the scale of the universe. The best that one can hope for is to gain information about the different local distributions of matter for various different samples of galaxies and clusters of galaxies at scales  $r \gg 1000h^{-1}\text{Mpc}$  and test them for homogeneity and isotropy (our Euclidean language is applicable locally in a curved space-time). If the scales required to exhibit evidence for homogeneity and isotropy should fall beyond the inherent limitations on all future observations, then the cosmological principle is not falsifiable and is only a matter of belief.

A more useful question is how to combine fractal or multifractal distributions with hydrody-

namics, now defining the density

$$\rho(\vec{x}) = \sum_{i=1}^N m_i \delta(\vec{x} - \vec{x}_i) \quad (44)$$

to include the masses of galaxies, as is done in part 6 of [13]. In a related publication [62] it is asserted that “. . . phenomena in which *intrinsic self-similar irregularities develop at all scales* and fluctuations cannot be described in terms of analytic functions. The theoretical methods used to describe this situation could not be based on ordinary differential equations because self-similarity implies the absence of analyticity and the familiar mathematical physics becomes inapplicable.” These claims are patently false: There is certainly no reason why one cannot study the dynamics of eq. (44) as an N-body problem using nonlinear differential equations, as was done by mathematicians from Laplace to Poincaré and beyond! Why was such a sweeping statement made to begin with? Clearly, by the extrapolation length scales to zero, to the empirically and physically meaningless mathematical limit where, essentially, two galaxies occupy the same position. Only in this limit are fractal densities nonanalytic enough to be completely nondifferentiable.

In fact the coarsegrained picture of empirical distributions formulated in parts 3.5 and 3.6 above leads in principle to a hydrodynamic description in terms of the usual differential equations of mathematical physics. At any desired resolution  $\approx l_n$ , simply represent the density by

$$\rho(\vec{x}) = \sum_{i=1}^{N_n} \rho_i \chi_{l_i}(\vec{x} - \vec{x}_i) \quad (45)$$

where (see eq. (44) above)  $\rho_i$  is the coarsegrained mass density for a partitioning  $\{l_i\}$ . One can certainly study the stability of this distribution (taken as an initial condition) via the usual differential equations of hydrodynamics, even if this may require solutions in the weak (or distribution) sense. The results will not be correct at length scales smaller than the scales  $\{l_i\}$ , but at smaller scales (down to  $l_{\min} > 0$ ) one can increase  $N_n$  (decreasing the size of intervals  $l_i$ ) and again study stability questions via a finer grained density of the form of (45). Uniform densities on space-filling supports in Newtonian cosmology are unstable if the universe is open, stable if the Euclidian manifold is a flat 3-torus [9]. In other words, homogeneity is globally unstable in an open Newtonian universe.

## 9 Platonic expectations?

The standard model of cosmology ([77], [61]) is a paradigm of simplicity: the simplest possible solution of Einstein’s field equations (global integrability based upon global symmetry) is combined with what Feynman has called “the usual initial conditions of physics”: random or thermal initial conditions. Feynman pointed out that biologists, geologists, and astronomers know that the usual initial conditions of physics (and integrable dynamics, one must add) cannot be used to explain most of the phenomena that are observed in nature ([22]). Cosmologically seen, far from equilibrium phenomena occur at relatively small scales. That these nonequilibrium nonuniformities at small scales should be consistent with perfect symmetry and random initial conditions at the largest scales is not at all clear. If it would be true then, as Plato [63] believed, the heavens would be perfect while all disorder is confined to the “sphere of the earth” (extended a bit, out to  $150 h^{-1}\text{Mpc}$ , at least).

It is not necessary to assume that the galaxy distribution requires the nineteenth century notion of randomness except perhaps as a sometimes convenient approximation to deterministic chaotic dynamics. We now understand how even the simplest chaotic dynamical systems can generate all possible historgams that can be constructed empirically ([53]). By randomness we mean a breakdown of the space-time description of cause and effect (as in quantum mechanics). Statistical independence ([38]), in contrast, is a separate idea that occurs in deterministic dynamics. Physics in the last twenty years has begun to follow more the path laid out by Poincaré ([54]), deviating

from the traditional path set down by Boltzmann (contrast the traditional emphasis on randomness found in [42] and in [81], for example, with the perspective on randomness expressed in [20]).

A deterministic dynamical system (like the differential equations that generate the characteristic curves of Newtonian or Einsteinian cosmology) can generate inhomogeneity that need not be fractal. A dynamical system far from thermodynamic equilibrium does not generate a unique probability distribution, but instead generates infinitely many different classes of distributions depending on classes of initial conditions. We would have no way to discover “the initial conditions of the universe” other than by accurate backward integrations in time starting from the present (empirically unknown) distribution of matter via the correct equations of motion. The laws of physics alone do not tell us anything about initial conditions ([79]). In the far from equilibrium case, on small scales, we know that mother nature has not chosen “the usual initial conditions of physics” (trees don’t grow from thermal equilibrium initial conditions, but arise instead from strong driving combined with dissipation).

Even if we knew the present cosmologic-scale distribution of matter the question whether the global matter distribution could have been generated from a thermally equilibrated initial state cannot be answered by N-body simulations, because no existing computer can reproduce, in backward integration in time, even the first digits of those initial conditions after integrations forward in time over billions of years. Accurate backward integrations were actually accomplished, for unknown reasons and for a very restricted range of energies, by building a special computer to try to simulate the evolution of the solar system via a chaotic symplectic map over millions of years ([71]). One object was to try to understand the initial conditions that initially fascinated Kepler<sup>1</sup>, the so-called Titius “law” (see also [78]).

The characteristic curves of the partial differential equations of Newtonian cosmology are generated by a dynamical system with a phase space of at least six dimensions (three degrees of freedom). The Lagrangian method [9] studies characteristics via backward integration in time, using the fact that initial conditions are trivially conserved along streamlines. Chaotic dynamics requires only a three dimensional phase space. Complex dynamics, dynamics equivalent to a universal computer (no scaling laws, no generating partition, nothing to aid in forecasting the future statistically) may occur in certain Newtonian systems with only three degrees of freedom ([58]). There, scaling laws, attractors, and the cardinality of strange sets can at best be defined only locally, if at all. It is unknown whether (any form of) fluid turbulence or the Newtonian three body problem fall into the complexity category. Expecting the universe to be describable by a completely integrable dynamical system, even at the largest scale of coarsegraining, seems unlikely in the light of what we now understand about deterministic dynamics. We are reminded that the cosmological principle is not demanded by any known laws of physics, and is not itself a separate law of nature.

This article was written with the benefit of hindsight. The author belongs to the subset of physicists who, in the past, has claimed evidence for  $\tau(q)$  on the basis of log-log plots that did satisfy the Geilo Criterion.

## Acknowledgement

I am very grateful to Martin Kerscher for generating the data analysis in Section 5, to Herbert Wagner and Thomas Buchert for criticism and discussions and to Herbert Wagner and Universität München for guestfriendship during Sept. – Feb. of my 1996–97 sabbatical year where I had the chance to learn some cosmology. The focus necessary to carry this project through was generated by the Oct. 1996 SchloßRingberg conference on cosmology. Thomas Buchert made it possible for me to attend that conference, while the encouragement to enter into the debate over fractals in galaxy statistics came from Herbert Wagner. We are grateful to Bernard Jones for some comments, and to Francesco Sylos-Labini and Luciano Pietronero for an exchange of ideas via email.

---

<sup>1</sup>Kepler was denied research support for his Platonic project to explain the initial conditions of the solar system on the basis of geometry alone ([10]).

## References

- [1] A. Anselmet, Y. Gagne, E.J. Hopfinger & R.A. Antonia, *J. Fluid Mech.* **140** (1984), 63.
- [2] E. Aurell, U. Frisch, J. Lutsko & M. Vergassola, *J. Fluid Mech.* **238** (1992), 467.
- [3] R. Badii & A. Politi, *Phys. Rev. Lett.* **52** (1984), 1661.
- [4] P. Bak, *How Nature Works, The Science of SOC*, Springer Verlag, Berlin, 1996.
- [5] A.-B. Barabasi & H.E Stanley, *Fractal Concepts in Surface Growth*, Cambridge University Press, Cambridge, 1995.
- [6] Y.V. Baryshev, F. Sylos-Labini, M. Montuori, & L. Pietronero, *Vistas in Astronomy* **38** (1994), 419–500.
- [7] C.M. Bender & S.A. Orszag, *Advanced Mathematical Methods for Scientists and Engineers*, McGraw–Hill, New York, 1995.
- [8] Stefano Borgani, Vicent J. Martinez, Miguel A. Perez & Riccardo Valdarnini, *Ap. J.* **435** (1994), 37–48.
- [9] Thomas Buchert & Jürgen Ehlers, *A&A* in press, astro-ph/9510056.
- [10] M. Caspar, *Johannes Kepler, tr. from German*, Dover Publications, New York, 1993.
- [11] C. Castagnoli & Provenzale, *Astron. Astrophys.* **246** (1991), 634.
- [12] B. Castaing, Y. Gagne & E.J. Hopfinger, *Physica* **D46** (1990), 177.
- [13] Paul H. Coleman & Luciano Pietronero, *Physics Rep.* **213** (1992), 311–389.
- [14] S. Columbi, F.R. Bouchet & Schaeffer, *Astron. Astrophys.* **263** (1992), 1.
- [15] A. Crisanti, M.H. Jensen, A. Vulpiani & G. Paladin, *Phys. Rev.* **A46** (1992), 7363.
- [16] P. Cvitanovic, G.H. Gunaratne & I. Procaccia, *Phys. Rev.* **A38** (1988), 1503.
- [17] M. Davis & P.J.E. Peebles, *Ap. J.* **267** (1983), 465.
- [18] M. de Sousa Viera & A.J. Lichtenberg, *Phys. Rev.* **E53** (1996), 1441.
- [19] K.J. Falconer, *Fractal Geometry*, John Wiley & Sons, Chichester, 1990.
- [20] M.J. Feigenbaum, *Los Alamos Science* **1** (1980), 4.
- [21] ———, *J. Stat. Phys.* **52** (1988), 527.
- [22] R.P. Feynman, F.B. Morinigo & W.G. Wagner, *Feynman Lectures on Gravity*, Addison-Wesley, Reading, MA, 1990.
- [23] Karl B. Fisher, John P. Huchra, Michael A. Strauss, Marc Davis, Amos Yahil & David Schlegel, *Ap. J. Suppl.* **100** (1995), 69.
- [24] U. Frisch, *Turbulence, The Legacy of A.N. Kolmogorov*, Cambridge University Press, Cambridge, 1995.
- [25] B.R. Gelbaum & J.H. Olmsted, *Counterexamples in Analysis*, Holden–Day, San Francisco, 1964.
- [26] J.A. Glazier, G. Gunaratne & A. Libchaber, *Phys. Rev.* **A37** (1988), 523.
- [27] P. Grassberger, R. Badii & A. Politi, *J. Stat. Phys.* **51** (1988), 135.

- [28] G.H. Gunaratne, *Universality beyond the onset of chaos in Chaos: Soviet and American Perspectives on Nonlinear Science* (New York) (D. Campbell, eds.), AIP, 1990.
- [29] G.H. Gunaratne & I. Procaccia, *Phys. Rev.* **A38** (1988), 1503.
- [30] T.C. Halsey, M.H. Jensen, L.P. Kadanoff, I. Procaccia & B.I. Shraiman, *Phys. Rev.* **A33** (1986), 1141.
- [31] H.G.E. Hentschel & I. Procaccia, *Physica* **D8** (1983), 435.
- [32] B. Hu, *Physics Rep.* **31** (1982), 233.
- [33] J. Huchra, M. Davis, D. Latham & J. Tonry, *Ap. J. Suppl.* **52** (1983), 89–119.
- [34] M.H. Jensen, L.P. Kadanoff & I. Procaccia, *Phys. Rev.* **A36** (1987), 1409.
- [35] B.J.T. Jones, *Nonlinear Galaxy Clustering*, *The Renaissance of General Relativity and Cosmology* (G.F.R. Ellis, A. Lanza & J. Miller, eds.), Cambridge University Press, Cambridge, 1996.
- [36] ———, *The Origin of Scaling in the Galaxy Distribution*; to appear in *MNRAS* (1997).
- [37] B.J.T. Jones, P. Coles & V.J. Martinez, *Mon. Not. R. Astron. Soc.* **259** (1992), 146–154.
- [38] M. Kac, *Carus Math. Monographs nr. 12: Statistical Independence in probability, analysis and number theory*, Wiley, New York, 1989.
- [39] L.P. Kadanoff, *Physica A* **163** (1990), 1–14.
- [40] L.P. Kadanoff, S.R. Nagel, L. Wu & S. Zhou, *Phys. Rev.* **A39** (1989), 6524.
- [41] Martin Kerscher, Jens Schmalzing, Thomas Buchert & Herbert Wagner, in preparation.
- [42] B. Mandelbrot, *The Fractal Geometry of Nature*, Freeman, San Francisco, 1982.
- [43] ———, *Proc. Roy. Soc. Lon.* **A434** (1991), 179.
- [44] V.J. Martinez, *Lecture Notes in Physics: Applying Fractals in Astronomy* (Berlin) (A. Heck & J. Perdang, eds.), Springer Verlag, 1991.
- [45] ———, *Proc. International School Enrico Fermi, Course CXXXII (Dark Matter in the Universe)*; in press.
- [46] V.J. Martinez & P. Coles, *Ap. J.* **437** (1994), 550.
- [47] V.J. Martinez & B.J.T. Jones, *Mon. Not. R. Astron. Soc.* **242** (1990), 517–521.
- [48] V.J. Martinez, B.J.T. Jones, R. Dominguez-Tenreiro & R. van de Weygaert, *Astron. Astrophys.* **357** (1990), 50.
- [49] V.J. Martínez, Silvestre Paredes, Stefano Borgani & Peter Coles, *Science* **269** (1995), 1245–1247.
- [50] V.J. Martinez & M.J. Pons, *Mapping, Measuring and Modelling the Universe* (San Francisco) (P. Coles, V.J. Martinez & M.-J. Pons-Bordeira, eds.), *Astron. Soc. of the Pacific*, 1996, pp. 241–246.
- [51] J.L. McCauley, *Physics Rep.* **189** (1990), 225.
- [52] ———, *Physica* **A197** (1993), 528.
- [53] ———, *Chaos, Fractals, and Dynamics: an algorithmic approach to deterministic chaos*, Cambridge University Press, Cambridge, 1993.

- [54] ———, *Classical Mechanics: Flows, Transformations, Integrability, and Chaos*, Cambridge University Press, Cambridge, 1997.
- [55] ———, to be published in *Physica A* (1997).
- [56] C. Meneveau & K.R. Srinivasan, *Phys. Rev. Lett.* **59** (1987), 1424.
- [57] ———, *J. Fluid Mech.* **224** (1991), 429.
- [58] C. Moore, *Phys. Rev. Lett.* **64** (1990), 2354.
- [59] K. Pawelzik & H.G. Schuster, *Phys. Rev.* **A35** (1987), 481.
- [60] Phillip J.E. Peebles, *The Large-Scale Structure of the Universe*, Princeton University Press, Princeton, New Jersey, 1980.
- [61] ———, *Principles of physical cosmology*, Princeton University Press, Princeton, New Jersey, 1993.
- [62] L. Pietronero, M. Montuori & F. Sylos-Labini, to appear in “Critical Dialogues in Cosmology”.
- [63] Plato, *Timaeus, tr. from Greek*, The Liberal Arts Press, N.Y., 1959.
- [64] R.Artuso, E. Aurell & P. Cvitanovic, *Nonlinearity* **3** (1990), 325.
- [65] R.Artuso, P. Cvitanovic & B.G. Kenney, *Phys. Rev.* **A39** (1989), 268.
- [66] H.L. Royden, *Real Analysis*, MacMillan Publ. Co., N.Y., 1968.
- [67] S. Sato, M. Sano & Y. Sawada, *Prog. Theor. Phys.* **77** (1987), 1.
- [68] P.E. Seiden & Schulman, *Adv. in Phys.* **39** (1990), 1.
- [69] Z.S. She, E. Aurell & U. Frisch, *Math. Phys.* **148** (1992), 623.
- [70] D. Stoyan, W.S. Kendall & J. Mecke, *Stochastic Geometry and its Applications*, John Wiley & Sons, Chichester, 1987.
- [71] G.J. Sussman & J. Wisdom, *Science* **257** (1992), 56.
- [72] F. Sylos Labini, A. Gabrielli, M. Montuori & L. Pietronero, *Physica A* **226** (1996), 195–242.
- [73] J. Theilor, *J. Opt. Soc. Am.* **A7** (1990), 1055.
- [74] R. van de Weygaert, B.J.T. Jones & V.J. Martinez, *Phys. Lett. A* **169** (1992), 145–150.
- [75] M. Vergassola, B. Dubrulle, U. Frisch & A. Noullez, *Astron. Astrophys.* **289** (1994), 325.
- [76] T. Viscek & Szalay, *Phys. Rev. Lett.* **58** (1987), 2818.
- [77] S. Weinberg, *Gravitation and Cosmology*, Wiley, New York, 1972.
- [78] C.F.v Weizsäcker, *Zeitschr. für Astrophys.* **22** (1944), 319.
- [79] E.P. Wigner, *Symmetries and Reflections*, Indiana Univ. Press, Bloomington, Ind., 1967.
- [80] X. Xia, Z. Deng & Z. Zou, *Science in China A* **35** (1992), 326.
- [81] Y.B. Zel’dovich, A.A. Ruzmaiken & D.D. Sokolov, *The Almighty Chance*, World Sc., Singapore, 1990.